



In silico screening of hundred phytochemicals of ten medicinal plants as potential inhibitors of nucleocapsid phosphoprotein of COVID-19: an approach to prevent virus assembly

Rajan Rolta^{a#}, Rohitash Yadav^{b#}, Deeksha Salaria^{a#}, Shubham Trivedi^c, Mohammad Imran^d, Anuradha Sourirajan^{a#}, David J. Baumler^e and Kamal Dev^a

^aFaculty of Applied sciences and Biotechnology, Shoolini University of Biotechnology and Management Sciences, Bajhol, Himachal Pradesh, India; ^bDepartment of Pharmacology, All India Institute of Medical Sciences, Rishikesh, Uttarakhand, India; ^cDepartment of Bioengineering, Integral University Lucknow, India; ^dDepartment of Pharmacology, Shaqra University, Saudi Arabia; ^eDepartment of Food Science and Nutrition, University of Minnesota—Twin Cities, St. Paul, Minnesota, USA

Communicated by Ramaswamy H. Sarma

ABSTRACT

Currently, there is no specific treatment to cure COVID-19. Many medicinal plants have antiviral, antioxidant, antibacterial, antifungal, anticancer, wound healing etc. Therefore, the aim of the current study was to screen for potent inhibitors of N-terminal domain (NTD) of nucleocapsid phosphoprotein of SARS-CoV-2. The structure of NTD of RNA binding domain of nucleocapsid phosphoprotein of SARS coronavirus 2 was retrieved from the Protein Data Bank (PDB 6VYO) and the structures of 100 different phytochemicals were retrieved from Pubchem. The receptor protein and ligands were prepared using Schrodinger's Protein Preparation Wizard. Molecular docking was done by using the Schrodinger's maestro 12.0 software. Drug likeness and toxicity of active phytochemicals was predicted by using Swiss adme, admetSAR and protox II online servers. Molecular dynamic simulation of the best three protein- ligand complexes (alizarin, aloe-emodin and anthrurufin) was performed to study the interaction stability. We have identified three potential active sites (named as A, B, C) on receptor protein for efficient binding of the phytochemicals. We found that, among 100 phytochemicals, emodin, aloe-emodin, anthrurufin, alizarine, and dantron of *Rheum emodi* showed good binding affinity at all the three active sites of RNA binding domain of nucleocapsid phosphoprotein of COVID-19. The binding energies of emodin, aloe-emodin, anthrurufin, alizarine, and dantron were -8.299 , -8.508 , -8.456 , -8.441 , and -8.322 Kcal mol⁻¹ respectively (site A), -7.714 , -6.433 , -6.354 , -6.598 , and -6.99 Kcal mol⁻¹ respectively (site B), and -8.299 , 8.508 , 8.538 , 8.841 , and 8.322 Kcal mol⁻¹ respectively (site C). All the active phytochemicals follows the drug likeness properties, non-carcinogenic, and non-toxic. These phytochemicals (alone or in combination) could be developed into effective therapy against COVID-19. From MD simulation data, we found that all three complexes of 6VYO with alizarin, aloe-emodin and anthrurufin were stable up to 50 ns. These phytochemicals can be tested further for *in vitro* or *in vivo* and used as a potential drug to cure SARS-CoV-2 infection.

ARTICLE HISTORY

Received 26 May 2020
Accepted 28 July 2020

KEYWORDS

RNA binding domain of nucleocapsid phosphoprotein; COVID-19; Molecular docking; Phytochemicals; antiviral and toxicity; Active site prediction and MD simulation

1. Introduction

During the end of year 2019, a venomous corona disease was emerged from the city of Wuhan, China (Baloch et al., 2020). In a short span of time, corona has spread all across the globe. This newly emerged viral disease was named as coronavirus disease (COVID-19 and also known as SARS-CoV-2) and World Health Organization (WHO) declared COVID-19 as global health emergency. The COVID-19 is transmitted through person to person and by so far has affected 213 countries across the World. Like other coronaviruses, SARS-CoV-2 has large genome (positive-sense, single-stranded RNA) size of around 30 kb, subdivided into 14 open reading frames (ORFs) (Gordon et al., 2020). The 5'-ORF 1a/ORF 1b

encodes for a polyprotein, which is further processed into 16 non-structural proteins (nsp1-16) by proteolytic cleavage (Gordon et al., 2020). The 3'- end of the RNA genome encodes for 13 ORFs for four structural proteins, such as the matrix (M), small envelope (E), spike (S) and nucleocapsid phosphoprotein (N), and facilitate entry of SARS-CoV-2 entry to human cells through human angiotensin converting enzyme 2 (ACE2) receptor (Gordon et al., 2020). Both structural and non-structural proteins ensure virus entry into the cells and its replication inside the host cell and therefore serve as potential as drug targets. The current antiviral drugs developed to treat coronavirus (CoV) infections primarily target S protein, the 3C-like (3CL), and papain-like (PLP)

CONTACT Kamal Dev  kamaldevbhardwaj1969@gmail.com  Professor, Faculty of Applied Sciences and Biotechnology, Shoolini University of Biotechnology and Business Management, Solan (HP), Bajhol, 173229, India
#Equal contribution.

 Supplemental data for this article can be accessed online at <https://doi.org/10.1080/07391102.2020.1804457>.

© 2020 Informa UK Limited, trading as Taylor & Francis Group

proteases (Ramajayam et al., 2011; Wrapp et al., 2020). The mutations in the S-protein could lead to escape of viral target by the drugs (Wrapp et al., 2020) whereas antiviral proteases could act on off targets and leads to potential side effects. Therefore, it is important to identify novel antiviral targets that could inhibit assembly of the virus particles. Viral nucleocapsid protein (N) is a potential antiviral drug target, serving multiple critical functions during the viral life cycle, including packaging the viral RNA genome (Baric et al., 1988; Cong et al., 2020; McBride et al., 2014; Nelson et al., 2000). The N-protein binds viral RNA genome and results in the formation of ribonucleoprotein (RNP) complex (Masters & Sturman, 1990; Nelson et al., 2000). The coronavirus N protein has distinct N-terminal RNA-binding domain (NTD), a C-terminal dimerization domain (CTD), and an intrinsically disordered central Ser/Arg (SR)-rich linker (Chen et al., 2013; Lo et al., 2013). It is been proposed that NTD is responsible for RNA binding protein and very crucial for transcription and replication of viral RNA (Grossoehme et al., 2009; Saikatendu et al., 2007). Many critical amino acid residues have been identified for RNA binding and virus infectivity in the N-terminal domain (NTD) of coronavirus N proteins (Tan et al., 2006). Therefore, NTD of nucleocapsid (N) protein RNA binding domains could be one of the essential drug targets to prevent assembly of virus particles (Kang et al., 2020).

Currently, there are really no approved drugs for the specific treatment of COVID-19. The COVID-19 is spreading at a much higher rate and the speed of drug discovery is quite slow and lengthy process. In order to speed up the process of drug development against COVID-19, there is an urgent need to take parallel and multidirectional approach to counter the spread of the virus. The approach to develop a vaccine from the scratch is a time taking process and not very good option for stopping an ongoing pandemic. The alternative approach is repurposing existing drugs such as remdesivir and chloroquine against COVID-19 could be a big step forward to curtail the growing threat (Sanders et al., 2020), but not yet approved by US-FDA for the treatment of COVID-19. This approach to new drug discovery against COVID-19 could be further boosted by *in silico* (hypothesis-based drug designing) approach and repurposing more existing FDA approved drugs (Ganjhu et al., 2015; Gupta, 2020). Moreover, phytochemicals of many medicinal plants have been traditionally used to cure many viral and respiratory diseases (Ben-Shabat et al., 2020; Ganjhu et al., 2015). Schwarz et al. (2011), specifically reported that emodin (major phytochemical of *Rheum emodi*) act as inhibitor of 3a ion channel of corona virus SARS-CoV and HCoV-OC43 as well as virus release from HCoV-OC4. Ho et al. (2007) identified emodin as an effective blocker of interaction of the SARS-CoV S protein with the ACE2 and the infection by S protein-pseudo-typed retrovirus. It was shown that the major phytochemicals of *Thymus serpyllum*, *Berberis aristata*, *Moringa oleifera*, *Zanthoxylum armatum*, *Piper nigrum*, *Myristica fragrans*, *Thalictrum foliolosum*, *Cymbopogon citrates* and *Allium sativum* are responsible for the antimicrobial, antiviral, antioxidant, anti-inflammatory, anti-HIV anti-carcinogenic properties (Aja et al., 2014; Fenwick & Hanley, 1985;

Ganjhu et al., 2015; Jaric et al., 2015; Meng et al., 1993; Naitan et al., 1993; Potdar et al., 2012; Sharma et al., 2020; Singh & Shikha, 2017; Takooree et al., 2019; Tsai et al., 1985; Oladeji et al., 2019; Weber et al., 1992).

In silico screening of such phytochemicals against specific targets of COVID-19 could provide a continuous feed for *in vitro* testing and clinical trials. Recently, Kang et al. (2020), solved the crystal structure of SARS-CoV-2 nucleocapsid protein RNA binding domain and proposed as unique target for developing therapeutics against COVID-19. Therefore, the current study was undertaken to test *in silico* inhibitory potential of 100 major phytochemicals of ten different medicinal plants including major phytochemicals of *R. emodi* against NTD of nucleocapsid protein RNA binding protein. The phytochemicals identified through *in silico* studies could become a feeder line for *in vitro* testing and clinical trials and therefore speed up the process of drug discovery against COVID-19 Figure 1.

2. Methods

2.1. Structure reliability of NTD of nucleocapsid phosphoprotein of SARS coronavirus 2

The structure of N-terminal domain (NTD, involved in RNA binding) of nucleocapsid phosphoprotein of SARS coronavirus 2 (N protein PDB ID: 6VYO; MMDB ID: 186265) was retrieved (<http://www.rcsb.org/structure/6VYO>; <https://www.ncbi.nlm.nih.gov> (Figure 3A) it based on the previous study by Yadav et al. (2020). The reliability of RNA binding domain of nucleocapsid phosphoprotein was done using the PROCHECK server, which displays Ramachandran plot with distinctive properties of protein such as most favored region, additional allowed regions, generously allowed regions, Disallowed regions, The End residues, Proline, Glycine and total number of residues. Multiple sequence alignment of SARS-N-terminal domain (NTD) of nucleocapsid phosphoprotein (6VYO) was done to find out the conserved regions.

2.1.1. Preparation of NTD of nucleocapsid phosphoprotein of SARS coronavirus 2 for docking

The three dimensional structure of RNA binding domain of nucleocapsid phosphoprotein from SARS coronavirus 2 (PDB ID: 6VYO) (global quality) was prepared using Schrodinger's Protein Preparation Wizard, by rectifying bond orders, addition of hydrogen bonds, making zero-order bonds to metal atoms, make disulphide bonds, making selenomethionine to methionine conversion, fill in lost side chains prime, erase waters from het groups, and generate het states using EpikPh 7 to +2 (Georgiev et al., 2005). Protein hydrogen bonds were optimized to remodel by the overlying hydrogen's and minimized using OPLS3e force field (Lanka et al., 2019).

2.1.2. Receptor grid generation and active sites prediction of NTD of nucleocapsid phosphoprotein of SARS coronavirus 2 for docking

Identification of the potential ligand binding sites or active site residues involved in interaction is a foremost step in

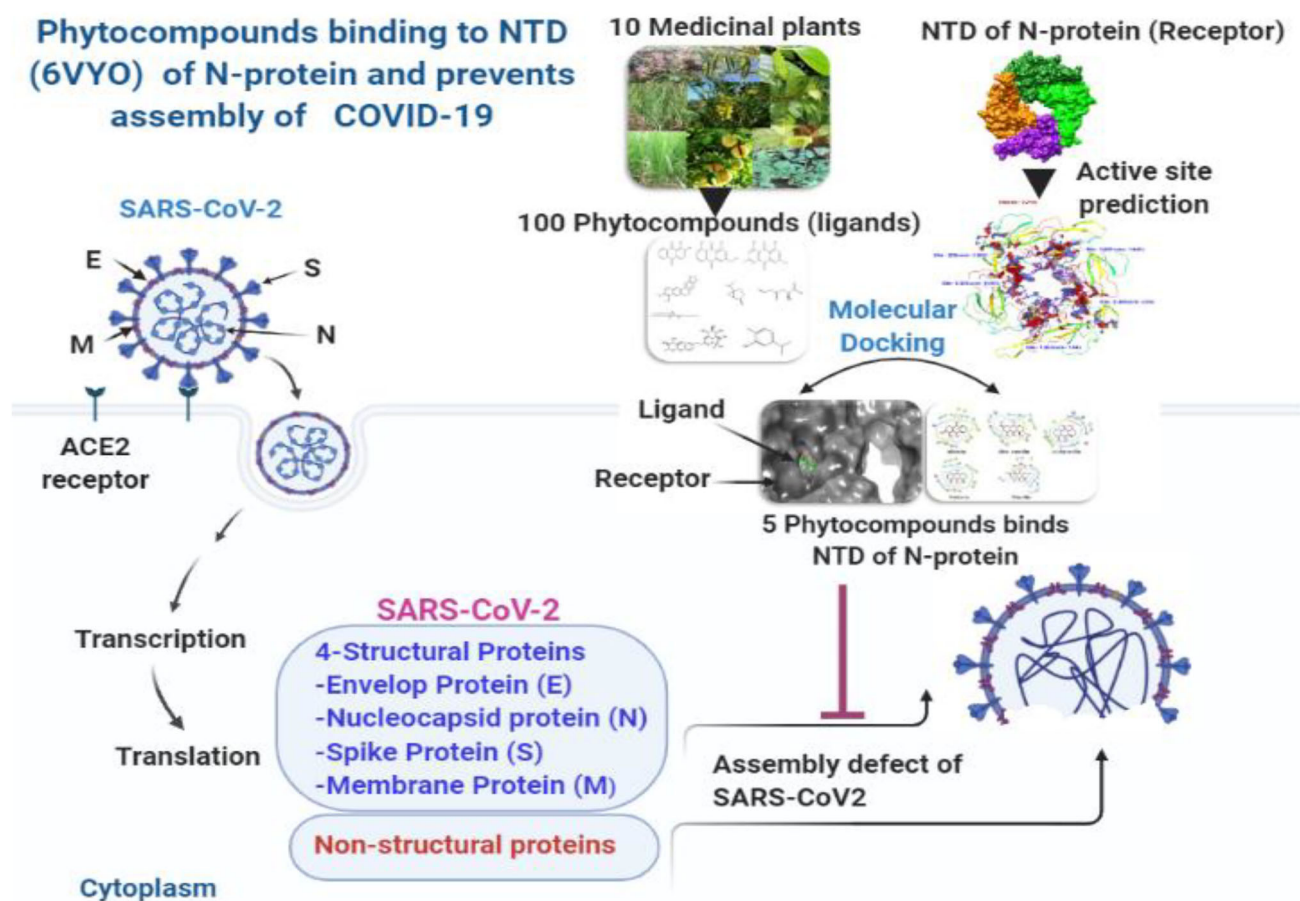


Figure 1. Proposed Binding mechanism of phytocompounds with NTD of nucleocapsid protein RNA binding protein of COVID-19 (Prepared using BioRender).

docking to discover novel chemical substances (Kalyaanamoorthy & Chen, 2011). The active site residues provide a pocket containing a variety of hydrogen donors, acceptors, hydrophilic regions and hydrophobic regions (Lionta et al., 2014). The binding cavity in NTD of nucleocapsid protein was identified using computational tools. Grid was generated using Glide module in Maestro 12.0 Schrodinger suite. The atoms of protein were settled inside using the default parameters of the radii of Vander Waal's scaling factor of 1 Å with partial charge cut-off of 0.25 Å using OPLS3e force field. Grid of the protein was generated by Yadav et al. (2020).

2.2. Preparation of phytocompounds (ligands)

Hundred major phytocompounds of ten medicinal plants (*Rheum emodi*, *Thymus serpyllum*, *Cymbopogon citrates*, *Moringa oleifera*, *Thalictrum foliolosum*, *Berberis aristata*, *Piper nigrum*, *Allium sativum*, *Myristica fragrans* and *Zanthoxylum armatum*) were utilized for virtual screening and molecular docking study against NTD of nucleocapsid (N-protein) of COVID-19 target proteins. All the hundred phytocompounds were retrieved from the PubChem Database (<https://pubchem.ncbi.nlm.nih.gov/>). Ligands were prepared by using the ligand preparation module of molecular modeling package with suitable parameters like optimization, ring conformation, 2D to 3D conversion, and determination of protomers, tautomers and ionization states at pH 7.0; along with partial

atomic charges using OPLS3e force field with root mean square deviation (RMSD) value of 0.11 Å.

2.3. Molecular docking

Molecular docking study of selected 100 phytocompounds of 10 medicinal plants for High throughput virtual screening was performed against the NTD of nucleocapsid N-protein (PDB ID: 6YVO). HTVS with flexible docking was performed on Schrodinger's maestro 12.0 between Ligands and active sites of target protein (6YVO). All the hundred ligands were filtered out by Standard Precision docking (SP) using ligand-docking process. Among hundred Ligands, the best configuration with highest docking score of virtual screening were sorted by Extra Precision (XP) with Flexible docking.

2.3.1. Binding free energies calculation using prime MM/GBSA approach

The binding free energies of ligand and receptor complex were analyzed by prime MM/GBSA (Molecular Mechanics Generalized Born Surface Area) module of Schrodinger suite with the OPLS3e force field. The prime MM GBSA⁻¹ approach is based on the docking complex and is used to calculate ΔG_{bind} of each ligand using the below mentioned equation- and as described earlier (Ramatenki et al., 2015; Tripathi et al., 2013).

$$\Delta G_{bind} = \Delta E_{MM} + \Delta G_{Solv} + \Delta G_{SA}$$

Where, ΔEMM is the difference in the minimized energies between the 6VYO-ligand complex and the sum of the energies of the unliganded 6VYO and inhibitor. ΔG_{Solv} is the difference in the GBSA solvation energy of 6VYO inhibitor complex and sum of the solvation energies for the free 6VYO receptor and inhibitor complex and ΔGSA is the difference in surface area energies for the complex and sum of the surface area energies for the unliganded 6VYO receptor and inhibitor. MM GBSA⁻¹ approach is used as a rescoring function to prioritize the lead inhibitors. The binding free energies obtained from MM GBSA¹ calculations were considered along with docking score to optimize the identified drug molecules.

2.4. Admet and toxicity prediction of active phytocompounds

Absorption, distribution, metabolism, excretion, and toxicity (ADMET) screening was done to determine the absorption, toxicity, and drug-likeness properties of ligands. The 3D structures of phytocompounds (aloe-emodin, anthrurufin, alizarine, dantron and emodin) were saved in .smiles format and drug were uploaded on SWISSADME (Molecular Modeling Group of the SIB (Swiss Institute of Bioinformatics), Lausanne, Switzerland), admetSAR (Laboratory of Molecular Modeling and Design, Shanghai, China), and PROTOX webservers (Charite University of Medicine, Institute for Physiology, Structural Bioinformatics Group, Berlin, Germany) for ADMET screening. SwissADME is a web tool used for the prediction of ADME and pharmacokinetic properties of a molecule. The predicted result consists of lipophilicity, water solubility, physicochemical properties, pharmacokinetics, drug-likeness, medicinal chemistry, and Brain or Intestinal Estimated permeation method (blood-brain barrier and PGP \pm prediction). admetSAR provides ADMET profiles for query molecules and can predict about fifty ADMET properties. Toxicity classes are as follows: (i) Category I contains compounds with LD₅₀ values $\leq 50 \text{ mg kg}^{-1}$, (ii) Category II contains compounds with LD₅₀ values $> 50 \text{ mg kg}^{-1}$ but 500 mg kg^{-1} but 5000 mg kg^{-1} . PROTOX is a Rodent oral toxicity server predicting LD₅₀ value and toxicity class of query molecule. The toxicity classes are as follows: (Class 1: fatal if swallowed (LD₅₀ ≤ 5), Class 2: fatal if swallowed (55000) (Banerjee et al., 2018).

MD Simulation

Molecular dynamic simulation was performed to analyze the stability of ligand-protein interactions with respect to the physical transition of the structural aspect of macromolecules to the functional relevance of the complex. In brief, MD simulation demonstrates strength, pattern, dynamic conformational changes and intermolecular properties of the interactions. Among all the complexes, best three complexes with binding site A were selected for MD simulation up 50 ns by using AMBER 18 software. The root mean square deviation (RMSD), root mean square fluctuation (RMSF), intermolecular hydrogen bonds interactions, binding

free energy and radius of gyration (RoG) were evaluated for the elucidation of conformational, structural and compactness of the protein-ligand complexes (Nandekar et al., 2013). Molecular receptor topology was created by leap module of software.

Subsequently, following established protocol such as neutralization and submerging complex into the water molecule rectangular box (TIP3P) where the protein atoms were 10 Å away from the nearest edge of the box. The minimization of the solvent system was achieved by freezing the protein and removing the bad contact with restraint on the heavy atoms, first through 2500 steepest descent method and then conjugation gradient for 2000 further steps. The system was gradually heated from 0 to 300 K temperature at 1 atm pressure (NPT conditions). It was achieved for 50 ps followed by 50 ps of density equilibrium and 1 ns of constant equilibrium to exchange the potential and kinetic energies. Afterward, the temperature was kept constant by using the Berendsen algorithm. The MDS was run for 50 ns to evaluate the stability of the docked ligand-receptor complexes preceded by the system equilibration for 500 ps on the canonical NPT ensemble. The covalently bound hydrogen atoms were constrained by the SHAKE algorithm with 2 fs time and temperature control by Langevin dynamics. Finally, the recording was made for every 5 ps using the particle-mesh Ewald summation method for treating electrostatic interaction. The RMSD, RMSF and RoG values were recorded for 50 ns.

3. Results

3.1. Protein structure reliability by ramachandran plot

The scheme for the current study has been summarized in Figure 2. The secondary structure of NTD (amino acid Ala 50 to Ala 173), the RNA binding domain of nucleocapsid phosphoprotein of SARS coronavirus 2 (6VYO) is shown in Figure 3A and secondary structure topology is shown in Figure 3B. The PROCHECK server presents Ramachandran plot displaying allowed and disallowed regions with regard to back bone dihedrals of protein residues. More than 90% score of the most favored regions ensures that model has good quality. RNA binding domain of nucleocapsid phosphoprotein of SARS coronavirus 2 (6VYO) protein showed 92.5% of amino acid residues in most allowed regions (Table 1 and Figure 3C). Multiple sequence alignment of SARS-N-terminal domain (NTD) of nucleocapsid phosphoprotein (6VYO) was done by blast to find out the conserved region. The domain hits showed similarity with Coronavirus nucleocapsid protein with E-value of 3.14×10^{-70} and with N-terminal domain of nucleocapsid (N) protein of coronavirus; The coronavirus nucleocapsid (N) with E-value of 1.23×10^{-54} (Figure 4A and B). The phylogenetic tree of RNA binding domain of nucleocapsid phosphoprotein from SARS coronavirus 2 is shown in supplementary Figure S1A and Multiple sequence alignment of nucleocapsid phosphoprotein from SARS coronavirus 2 in supplementary Figure S1B.

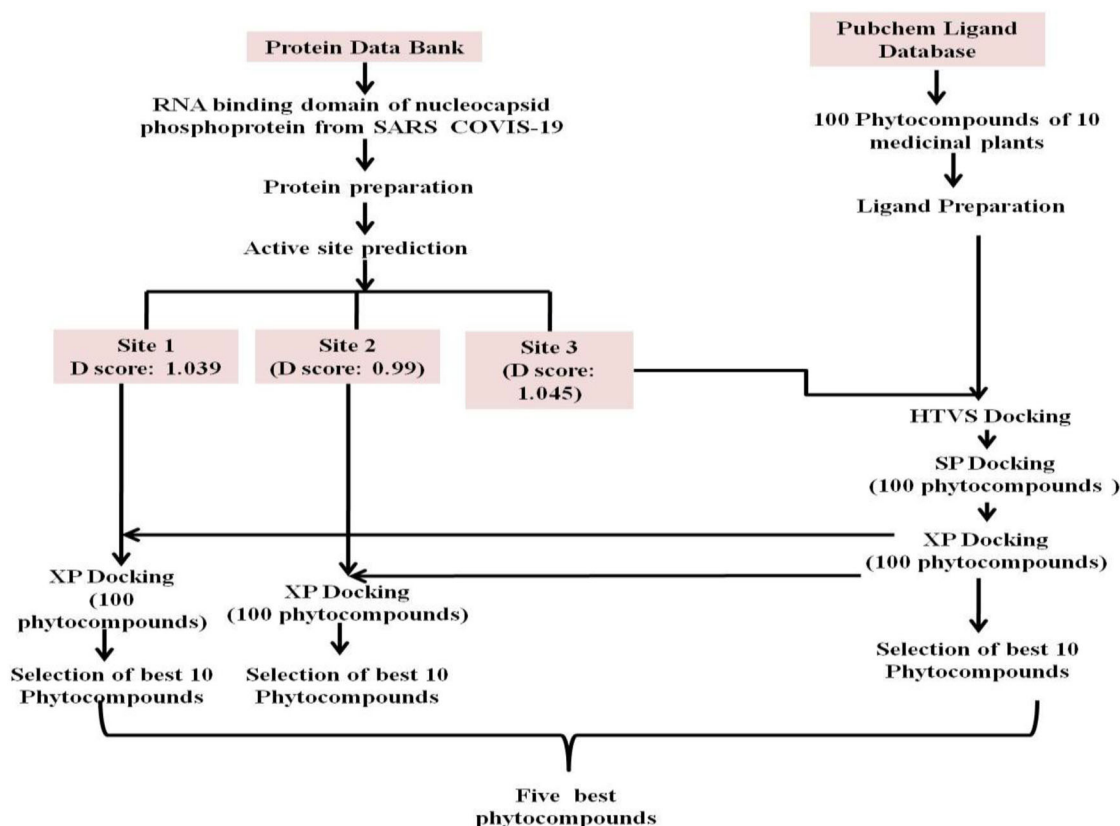


Figure 2. Schematic of the experiments followed in the current study.

3.1.2. Preparation of NTD, the RNA binding domain of nucleocapsid phosphoprotein of SARS coronavirus 2 (6VYO)

The three dimensional homo-tetrameric structure of RNA binding domain of nucleocapsid phosphoprotein of SARS coronavirus 2 (PDB ID: 6VYO) was retrieved from RCSB PDB (<http://www.rcsb.org/pdb>) in .sdf format. The protein structure was prepared by correcting bond orders, addition of hydrogen bonds, creating zero-order bonds to metal atoms, creating disulphide bonds, creating selenomethionine to methionine conversion, fill in the missing side chains prime, deleting waters from het groups, and generate het states using EpikPh 7 to +2 by using Schrodinger's Protein Preparation Wizard (Figure 5A-D).

3.1.3. Receptor grid generation and active site prediction

To predict the active site of RNA binding domain of nucleocapsid phosphoprotein from SARS coronavirus 2 (PDB ID: 6VYO), protein grid was generated by using glid module in maestro 12.0 schrodinger suit. In RNA binding domain of nucleocapsid phosphoprotein from SARS coronavirus 2 (PDB ID: 6VYO) protein, we found three different active sites, namely A, B and C with D score 1.039, 0.99 and 1.045 respectively. Active site of target protein is based on previous study Yadav et al. (2020). The dimensions of the grid box and receptor setup were $x=80\text{ \AA}$, $y=80\text{ \AA}$, $z=80\text{ \AA}$ and $x=32\text{ \AA}$, $y=32\text{ \AA}$, $z=32\text{ \AA}$ respectively with a grid space of 1 \AA for all the three binding

sites. Active site A was predicted between chain A and B. The chain A contributes 26 amino acid and chain B contributes 21 amino acids. The Active site B was predicted between chain A (25 amino acids) and chain B (26 amino acids). Active site C was predicted between chain C and D with 15 and 21 amino acids respectively (Table 2 and Figure 5 A-D). This is important to mention that Thr 76, Ser 78, Ser 105, Thr 166 which are potential phosphorylation sites are involved in formation of active sites A, B and C (Table 2; Yadav et al., 2020).

3.2. Ligand preparation

Hundred major phytocompounds of ten selected medicinal plants (*Rheum emodi*, *Thymus serpyllum*, *Cymbopogon citratus*, *Moringa oleifera*, *Thalictrum foliolosum*, *Berberis aristata*, *Piper nigrum*, *Allium sativum*, *Myristica fragrans* and *Zanthoxylum armatum*) were used for the docking studies. The 3-dimensional structures of all the phytocompounds were obtained from pubchem (www.pubchem.com) in .sdf format. The .sdf file of phytocompounds was converted into PDB format by using the tool Open Babel. Table 3 summarizes the names of the medicinal plants, pharmacological properties and major phytocompounds. Phytocompounds are numbered as 1-100. Figure 6 showed five phytocompounds of *R. emodi*, which showed very efficient binding with NTD of nucleocapsid phosphoprotein of SARS coronavirus 2.

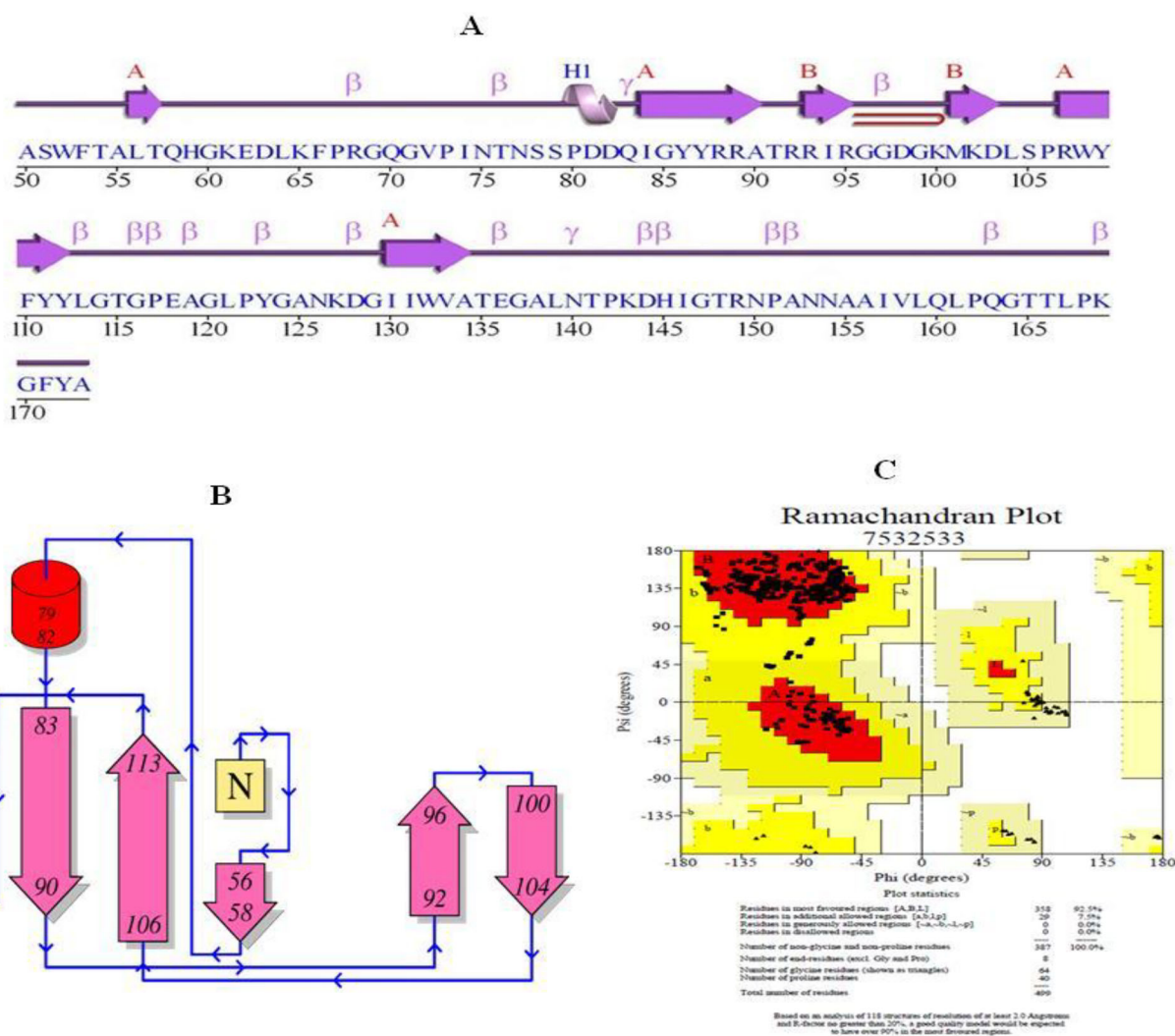


Figure 3. (A) Secondary structure of NTD (amino acid residues 50-173) of RNA binding domain of nucleocapsid phosphoprotein from SARS coronavirus 2 (PDB ID: 6VYO); (B) Topology of secondary structure; and (C) The Ramachandran plot describes the favored and disfavored regions of residues. The maximum (92.5%) residues are located in an allowed region.

Table 1. Ramachandran Plot statistics showing favored regions in RNA binding domain of nucleocapsid phosphoprotein from SARS coronavirus 2 (PDB ID: 6VYO) (Yadav et al., 2020).

Properties	RNA binding domain of nucleocapsid phosphoprotein from SARS coronavirus 2(6VYO)	
	Residues	%
The Most favored regions	358	92.5
Additional allowed regions	29	7.5
Generously allowed regions	0	0
Disallowed regions	0	0
The End residues (excluding Glycine and Proline)	8	-
Proline	64	-
Glycine	40	-
Total number of residues	499	100

3.3. Molecular docking analysis of RNA binding domain of nucleocapsid phosphoprotein from SARS coronavirus 2 (PDB ID: 6VYO) target protein and phytocompounds

Molecular docking of all the 100 phytocompounds with three binding sites (A, B and C) of RNA binding domain of

nucleocapsid phosphoprotein from SARS coronavirus 2 (PDB ID: 6VYO) protein was done by using Schrodinger's Software. Active phytocompounds were analyzed by scoring function and binding free energies MM GBSA⁻¹. Out of the hundred phytocompounds, only five phytocompounds showed the best interactions with all three-binding site of RNA binding domain of nucleocapsid phosphoprotein from SARS coronavirus 2 (PDB ID: 6VYO) protein (Tables 4–6 and Figures 7–12). Molecular structures of five best phytocompounds are shown in Figure 6. The remaining 95 phytocompounds did not show efficient binding (data not shown) and hence were not pursued further.

3.3.1. Molecular docking of phytocompounds with active site A

Active site A was predicted between chain A and Chain B with D score 1.039. Among all the selected phytocompounds, only aloe-emodin, anthraruflin, alizarine, dantron and emodin showed the best interaction with docking score -8.508 , -8.456 , -8.441 , -8.322 and -8.299 Kcal mol⁻¹ respectively. Prime MM GBSA⁻¹ (Kcal mol⁻¹), hydrogen

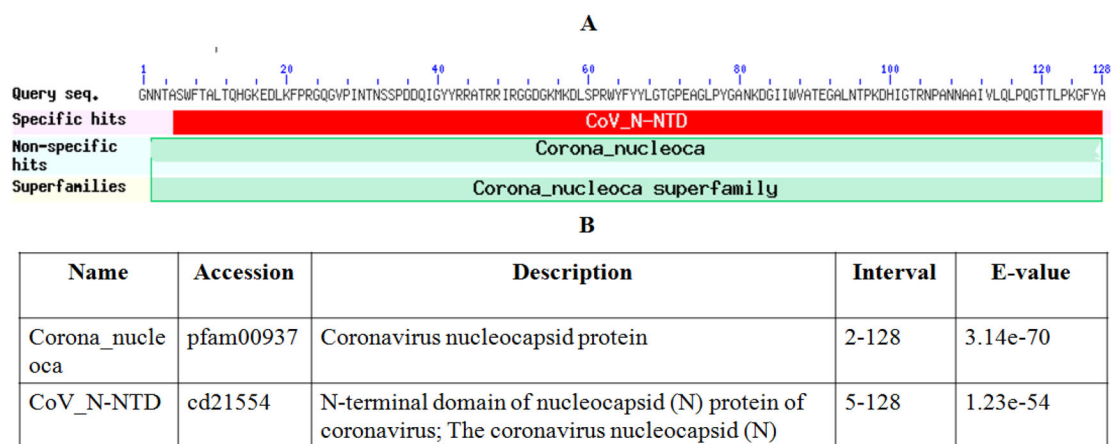


Figure 4. (A) Conserved domains of (6 VYO_1) chains A, B, C, D nucleoprotein of Severe acute respiratory syndrome coronavirus 2. (B) List of domain hits with E-values.

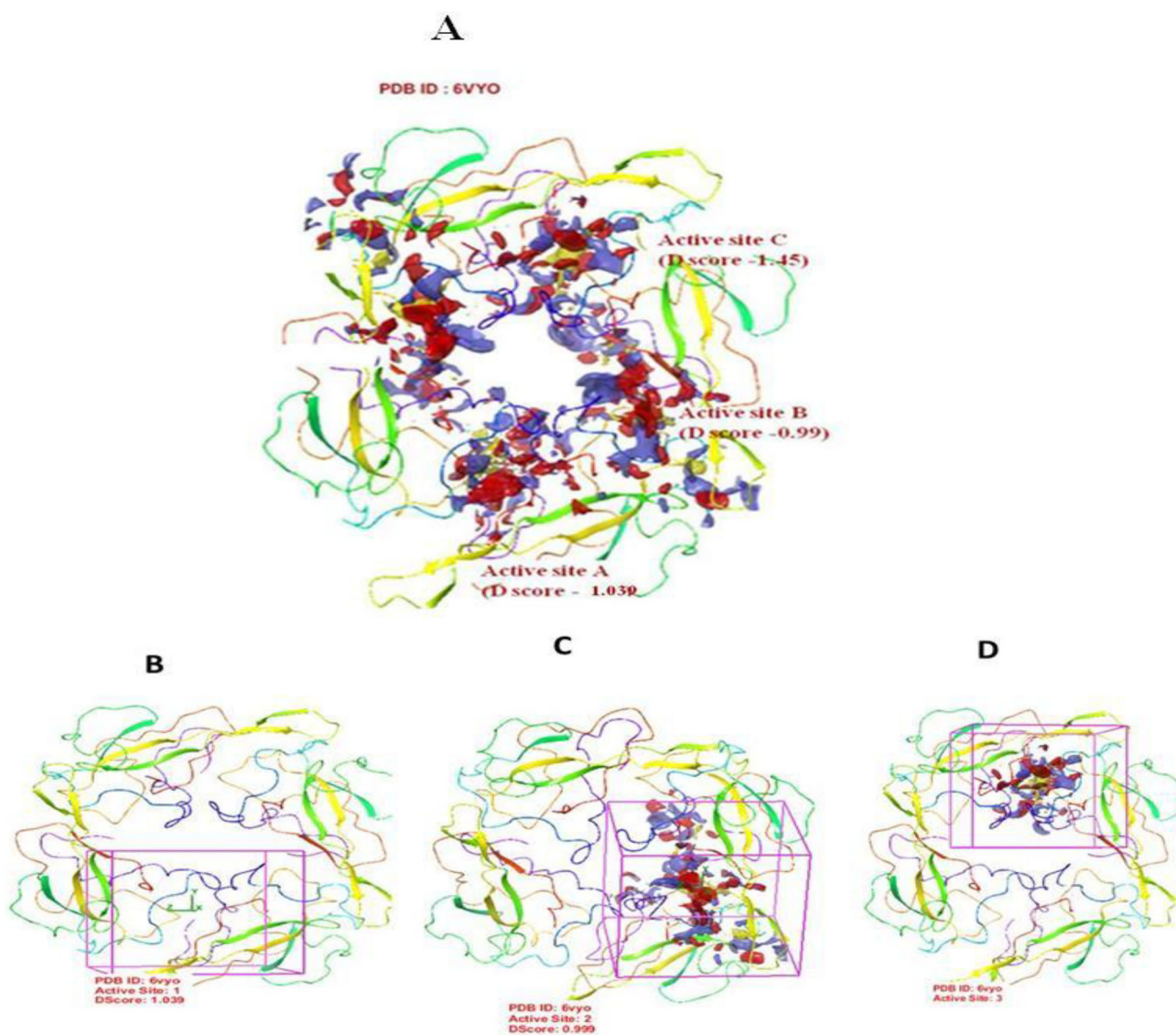


Figure 5. Active site prediction. 3-D structure representation of tetrameric RNA binding domain (N-terminal domain) of nucleocapsid phosphoprotein from SARS coronavirus 2 (PDB ID: 6VYO) showing three predicted binding sites shown as Active site A, Active site B and Active site C (A). Panel B, C, and D represent tetrameric RNA binding domain showing each active site as indicated.

Table 2. Amino acids involved in active sites of RNA binding domain of nucleocapsid phosphoprotein from SARS coronavirus 2 (PDB ID: 6VYO) (Yadav et al., 2020).

Active Sites	D Score	Size	Site Score	Chains and amino acid residues numbers
Site-A	1.039	216	1.009	CHAIN A: ALA 50, SER 51, PHE 53, THR 54, ALA 55, LEU 56, THR 57, HIP 59, ARG 92, SER 105 , ARG 107, TYR 109, ARG 149, ALA 156, ILE 157, VAL 158, GLN 160, LEU 161, PRO 162, GLN 163, GLY 164, THR 165, LEU 167, PHE 171, TYR 172, ALA 173 CHAIN B: TRP 52, PHE 53, PRO 73, ILE 74, ASN 75, THR 76 , ASN 77, SER 78 , ASP 82, HIE 145, ILE 146, THR 148, ARG 149, ASN 150, ASN 153, ASN 154, ALA 155, VAL 158, LEU 159, GLN 160, ILE 157
Site-B	0.99	196	0.98	CHAIN A: TPR 52, PHE 53, PRO 73, ILE 74, ASN 75, THR 76 , ASN 77, TYR 112, GLY 114, THR 115, GLY 116, ALA 119, ASP 144, HIE 145, ILE 146, GLY 147, THR 148, ARG 149, ASN 150, ASN 153, ASN 154, ILE 157, VAL 158, LEU 159, GLN 160 CHAIN D: THR 54, ALA 55, THR 57, HIE 59, ALA 90, THR 91, ARG 92, ILE 94, GLY 96, GLY 97, ASP 98, LYS 102, LEU 104, SER 105 , PRO 106, ARG 107, TYR 109, VAL 158, LEU 159, GLN 160, LEU 161, GLN 163, THR 165, THR 166 , LEU 167, ALA 173
Site-C	1.045	183	1.039	CHAIN C: ALA 50, SER 51, PHE 53, THR 54, ALA 55, LEU 56, THR 57, HIP 59, ARG 92, ARG 107, TYR 109, ARG 149, ALA 156, ILE 157, VAL 158 CHAIN D: TRP 53, PRO 73, ILE 74, ASN 75, THR 76 , ASN 77, SER 78 , ASP 82, HIE 145, ILE 146, GLY 146, THR 148, ARG 149, ASN 150, ASN 153, ASN 154, ALA 155, ILE 157, VAL 158, LEU 159, GLN 160

Each amino acid residue is numbered followed by three letter code. Amino acid residues in boldface letters are the phosphorylation sites on Serine and Threonine were predicted by Davidson et al. (2020). Nonstandard amino acids are CL, GOL, HOH, MES, ZN.

Table 3. List of hundred major phytochemicals (numbered 1-100) of 10 medicinal plants with pharmacological properties.

S.No	Medicinal Plants	Pharmacological properties	Major phytochemicals Selected for the current study
1.	<i>Rheum emodi</i>	Treatment of Severe Acute Respiratory Syndrome (SARS) (Ho et al., 2007; Schwarz et al., 2011). Antioxidant, antibacterial antifungal and Bioenhancer of antibiotics (Dev et al., 2017; Rolta et al., 2018a; 2020).	(1) Alizarin, (2) Aloe-emodin, (3) Anthraquinone, (4) Anthrarufin, (5) Anthrone, (6) Chrysoferol, (7) Clicoemodin, (8) Dantron, (9) Emodin, (10) Gallic acid, (11) Juglone, (12) Physicon, (13) Piceatannol, (14) Quinizarin, (15) Rubiadin
2.	<i>Thymus serpyllum</i>	Antimicrobial, antiviral, antioxidant, anti-inflammatory and anti-carcinogenic (Jaric et al., 2015)	(16) 3-Octanone, (17) 8-PrenylNaringenin, (18) Apigenin, (19) Apigenin-7-O-glucoside, (20) Bornyl acetate, (21) Camphene, (22) Camphor, (23) Carvacrol, (24) Caryophyllene oxide, (25) Catechin, (26) Eriodictyol, (27) Eriodictyol-7-glucuronide, (28) Geranyl acetate, (29) Linalool, (30) Myrcene, (31) Rutin, (32) Spathulenol, (33) Taxifolin, (34) Thymol, (35) trans-Nerolidol, (36) α -Pinene, (37) β -Bisabolene, (38) β -Caryophyllene, (39) β -Pinene, (40) δ -Cadinene.
3.	<i>Cymbopogon citrates</i>	Anti-obesity, anti-bacterial, anti-fungal, anti-nociceptive, anti-oxidants anti-diarrheal, and anti-inflammatory (Singh & Shikha, 2017).	(41) Citral alpha, (42) citronellal, (43) Geraniol, (44) lemonene, (45) nerol, (46) terpinolene
4.	<i>Moringa oleifera</i>	Antimicrobial (Pal et al., 1995) antiviral potential (Aja et al., 2014).	(47) Glucomoringin, (48) Niazinin A, (49) Niazinin, (50) Pterygospermin
5.	<i>Thalictrum foliolosum</i>	Antiplasmodial, antiviral, antibacterial and anti-gastric ulcer activity (Sharma et al., 2020)	(51) 8-Oxyberberine, (52) Berberine, (53) Jatrorrhizine, (54) Noroxyhydrastinine, (55) Palmatine, (56) Thalicarpine, (57) Thalidasine, (58) Thalarugidine, (59) Thalarugine, (60) Thalispine, (61) Thalrugosaminine, (62) Thalrugosidine
6.	<i>Berberis aristata</i>	Anti-diabetic, anti-microbial, anti-cancer, antilipidemic, anti-HIV, anti-pyretic (Potdar et al., 2012)	(63) Berbamine, (64) Columbamine, (65) Isocorydine, (66) Lambertine, (67) Lupeol, (68) Oleanolic acid, (69) Oxyberberine, (70) Oxycanthine, (71) Stigmasterol
7.	<i>Piper nigrum</i>	Antimicrobial, antioxidant, anticancer, analgesic, anticonvulsant, neuroprotective, hypoglycemic, hypolipidemic, and anti-inflammatory activities (Takooree et al., 2019)	(72) Sabinene, (73) Piperolein B, (74) Piperolein A, (75) Piperine, (76) Piperazine, (77) Guaiol, (78) β -caryophyllene
8.	<i>Allium sativum</i>	Anti-influenza A and B (Fenwick & Hanley, 1985), antiviral (Meng et al., 1993; Nai-Lan et al., 1993; Tsai et al., 1985)	(79) Vinylolithium, (80) Alliin, (81) Allicin, (82) (Z)-Ajoene, (83) (E)-Ajoene
9.	<i>Myristica fragrans</i>	Antioxidant, antimicrobial, aphrodisiac, anticancer, hepatoprotective, anti-inflammatory, antidepressant, and cardioprotective activity (Ganjhu et al., 2015)	(84) Trimyrustin, (85) saffrole, (86) Sabinene, (87) myristicin, (88) methoxyeugenol, (89) meso-dihydroguaiaretic acid, (90) isoelemicin, (91) elemicin, (92) camphene, (93) 9-epoxy lignan, (94) 4-terpinol
10.	<i>Zanthoxylum armatum</i>	Antifungal, antibacterial, antiviral, anti-inflammatory, anti-oxidant, cardiovascular and immunomodulatory (Singh & Shikha, 2017)	(95) β -Sitosterol- β -D-Glucoside, (96) Xanthyletin, (97) Tambulin, (98) Sesamin, (99) Bergapten, (100) Armatamide

bonding and interactive amino acids are shown in Table 4, Figures 7 and 8. Apart from hydrophobic interactions, H-bonds were also detected. Ser 78 of chain B, which has been predicted as phosphorylation site showed interaction with all the five phytochemicals.

3.3.2. Molecular docking of phytochemicals with active site B

Active site B was predicted between chain A and chain With D score 0.99. Among all the selected phytochemicals, only emodin, dantron, alizarine, aloe-emodin and anthrarufin

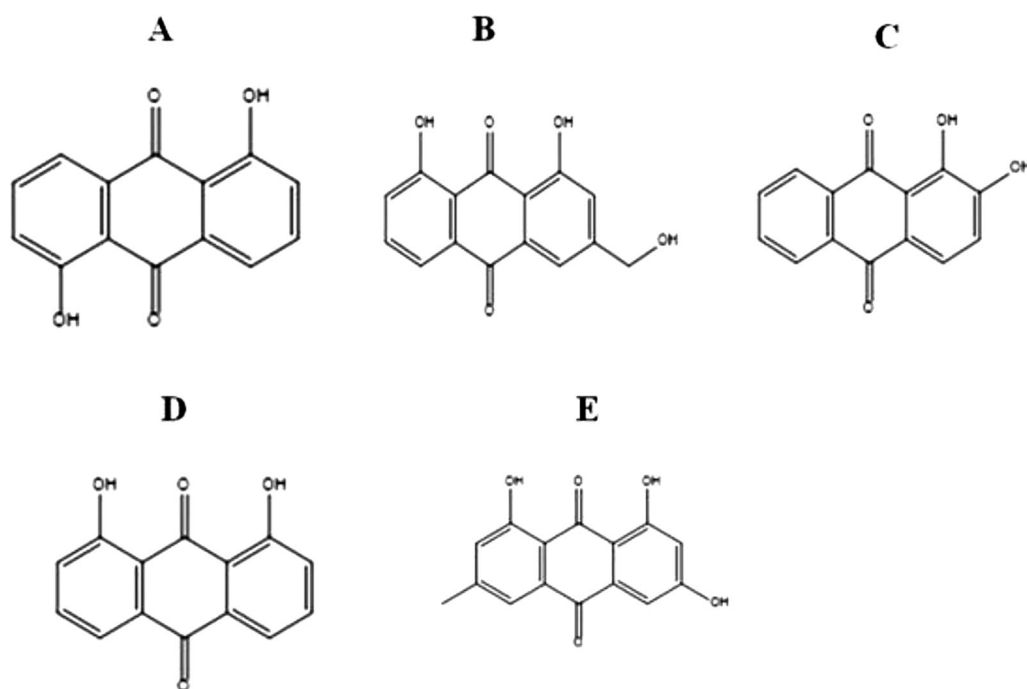


Figure 6. Structures of potential phytocompounds of *R. emodi*: A) Anthrarufin, (B) Aloe- emodin, (C) Alizarine, (D) Dantron, (E) Emodin.

TABLE 4. Interacting amino acids and docking score of phytocompounds with binding site A (1.039) of 6VY0.

Compound CID no.	Name of Ligand (Plant source)	ΔG Bind (kcal mol ⁻¹)	Docking Score	H-bond	Interactive Residues
10207	Aloe- emodin (<i>Rheum emodi</i>)	-25.45	-8.508	Chain A: ARG 107 Chain B: HIE 145, ASN 75, ASN 77	Chain A: LEU 159, VAL 158, THR 54, ALA 55, THR 57, HIP 59, ARG 92, ARG 107 Chain B: SER 78, ILE 157, ASN 154, TRP 52, ILE 146, HIE 145, ASN 75, ASN 77
8328	Anthrarufin (<i>Rheum emodi</i>)	-38.099	-8.456	Chain B: ASN 75	Chain A: THR 54, ALA 55, THR 57, HIP 59, ARG 92, ARG 107, VAL 152 Chain B: TRP 52, ASN 154, ILE 157, ASN 77, SER 78, ILE 146, HIE 145, ASP 82, ASN 75
6293	Alizarine (<i>Rheum emodi</i>)	-31.2891	-8.441	Chain A: ASN 75 Chain B: ASN 77, ASN 75, HIE 145	Chain A: ARG 107, HIP 59, ARG 92, ALA 55, THR 54, LEU 159, VAL 158, ASN 75 Chain B: TRP 52, TYR 112, ILE 157, ASN 154, SER 78, ILE 146, HIE 145, ASN 77, ASN 75
2950	Dantron (<i>Rheum emodi</i>)	-39.8129	-8.322	Chain A: THR 57, ALA 55 Chain B: ASN 75, ASN 77	Chain A: HIP 59, LEU 56, THR 54, ARG 107, LEU 159, VAL 158, THR 57, ALA 55 Chain B: ASP 82, HIE 145, ILE 146, SER 78, TRP 52, ILE 157, ASN 75, ASN 77
3220	Emodin (<i>Rheum emodi</i>)	-43.87	-8.299	Chain A: ALA 55 Chain B: ASN 77, ASN 75	Chain A: VAL 158, LEU 159, THR 54, LEU 56, HIP 59, ARG 107, ALA 55 Chain B: ASP 82, ILE 157, TRP 52, SER 78, HIE 145, ILE 146, ASP 82, ASN 77, ASN 75

Each amino acid residue is numbered followed by three letter code. Amino acid residues in boldface letters are the phosphorylation sites on Serine and Threonine were predicted by Davidson et al. (2020).

showed the best interaction with docking score -7.714 , -6.99 , -6.598 , -6.433 and -6.354 Kcal mol⁻¹ respectively. Prime MM GBSA⁻¹ (Kcal mol⁻¹), hydrogen bonding and interactive amino acid is shown in Table 5, Figures 9 and 10. Both hydrophobic and H-bond interactions were observed. Ser 78 of Chain A and Ser 105 of chain B, the potential phosphorylation residues were also involved in hydrophobic interaction. Exceptionally, SER 78 of chain A also showed H-bond formation with Aloe-emodin.

3.3.3. Molecular docking of phytocompounds with active site C

Active site C was predicted between chain A and chain d with D score 1.045. Among all the selected phytocompounds, anthrarufin, aloe-emodin, alizarine, dantron and emodin showed the best interaction with docking score -8.538 , -8.508 , -8.841 , -8.322 and -8.299 Kcal mol⁻¹ respectively. Prime MM GBSA⁻¹ (Kcal mol⁻¹), hydrogen

Table 5. Interacting amino acids and docking score of phytochemicals with binding site B (0.99).

Compound CID no.	Name of Ligand (Plant source)	ΔG Bind (kcal mol ⁻¹)	Docking Score	H-bond	Interactive Residues
3220	Emodin (<i>Rheum emodi</i>)	-40.60	-7.714	Chain A: HIE 145, ASN 77, ASN 75, ASN 154 Chain D: ARG 92	Chain A: ILE 146, SER 78 , TRP 52, ILE 157, HIE 145, ASN 77, ASN 75, ASN 154 Chain D: HIE 59, ALA 173, THR 57, LEU 104, SER 105 , ARG 107, ARG 92
2950	Dantron (<i>Rheum emodi</i>)	-45.48	-6.99	Chain A: ASN 154, ILE 146, ASN 77	Chain A: TRP 52, ASN 75, ULE 157, HIE 145, ASN 75, SER 78 , ASN 154, ILE 146, ASN 77 Chain D: ARG 107, SER 105 , LEU 104, ARG 92
6293	Alizarine (<i>Rheum emodi</i>)	-33.59	-6.598	Chain A: ASN 77, ASN 75	Chain A: ILE 146, HIE 145, ARG 92, SER 78 , TRP 52, ILE 157, ASN 154, ASN 77, ASN 75 Chain D: SER 105 , ARG 107, HIE 59, THR 57
10207	Aloe- emodin (<i>Rheum emodi</i>)	-36.92	-6.433	Chain A: ASN 154, ILE 157, SER 78 , ILE 146, HIE 145, TRP 52, ASN 75, ASN 77	Chain A: ASN 154, ILE 157, SER 78 , ILE 146, HIE 145, TRP 52, ASN 75, ASN 77 Chain D: ARG 107, SER 105 , LEU 104, ARG 92, HIE 59, THR 57
8328	Anthrarufin (<i>Rheum emodi</i>)	-34.9567	-6.354	Chain A: ASN 77	Chain A: SER 78 , ASN 75, TRP 52, ILE 146, ILE 157, ASN 77 Chain D: ARG 107, SER 105 , ARG 92, THR 57, HIE 59

Each amino acid residue is numbered followed by three letter code. Amino acid residues in boldface letters are the phosphorylation sites on Serine and Threonine predicted by Davidson et al. (2020).

Table 6. Interacting amino acids and docking score of phytochemicals with binding site-C (1.045).

Compound CID no.	Name of Ligand (Plant source)	ΔG Bind (kcal mol ⁻¹)	Docking Score	No. of H-bond	Interactive Residues
8328	Anthrarufin (<i>Rheum emodi</i>)	-39.48	-8.538	Chain D: ASN 75, ASN 77	Chain C: TTR 54, ALA 55, THR 57, HIP 59, ARG 107, ARG 92 Chain D: TRP 52, ASN 154, ILE 157, HIS 145, ILE 146, SER 78 , ASP 82, ASN 75, ASN 77
10207	Aloe- emodin (<i>Rheum emodi</i>)	-32.61	-8.508	Chain C: THR 57, LEU 159 Chain D: ASN 75	Chain C: HIP 59, LEU 56, ALA 55, THR 54, VAL 158, LEU 159, THR 57, LEU 159 Chain D: ASN 77, SER 78 , ASN 154, ILE 157, VAL 158, LEU 159, ILE 146, HIS 145, ARG 107, ASN 75, ASN 75
6293	Alizarine (<i>Rheum emodi</i>)	-33.84	-8.441	Chain C: ALA 55, LEU 56, THR 57 Chain D: ASN 75	Chain C: THR 54, LEU 159, VAL 158, ALA 55, LEU 56, THR 57 Chain D: HIS 145, ILE 146, ASN 77, SER 78 , ASN 154, ILE 157, TRP 52, TYR 112, ASN 75
2950	Dantron (<i>Rheum emodi</i>)	-35.459	-8.322	Chain C: THR 57, ALA 55	Chain C: HIP 59, THR 57, LEU 56, ALA 55, THR 54, ARG 107, VAL 158, LEU 159 Chain D: HIS 145, ILE 146, TRP 52, SER 78 , ASN 77, ASN 154, ILE 157, ASP 82
3220	Emodin (<i>Rheum emodi</i>)	-32.78	-8.299	Chain C: ARG 107 Chain D: ILE 146, ASN 175	Chain C: TYR 109, ARG 107, ARG 92, HIP 59, THR 57, ALA 55, THR 57 Chain D: ASN 153, ASN 154, ILE 146, HIS 145, TRP 52, ASP 82, SER 79 , SER 77, ASN 75

Each amino acid residue is numbered followed by three letter code. Amino acid residues in boldface letters are the phosphorylation sites on Serine and Threonine predicted by Davidson et al. (2020).

bonding and interactive amino acid is shown in Table 6, Figures 11 and 12. Hydrophobic interactions and H-bonds were detected all the phytochemicals. Ser 78 of chain D, the potential phosphorylation residue was also involved in hydrophobic interaction.

3.4. Admet prediction and toxicity analysis of active phytochemicals

The ADME properties predicted by SwissADME of selected phytochemicals are summarized in Table 7. Consensus Log

Po/w value of <5 indicates good aqueous solubility, which means that an adequate amount of drug can reach the target and can be maintained inside the body through oral administration. All the five phytochemicals have consensus Log Po/w value of <5 (Table 7). TPSA indicates a compound ability to permeate into cells. A TPSA value of <140 Å² is required for good permeation of compound into the cell membrane and value <90 Å² is required to permeate through blood-brain barrier. All the selected phytochemicals have TPSA value <90 Å², indicating good permeability of selected phytochemicals through blood-brain barrier. Lipinski's rule of five helps to determine drug-likeness of the

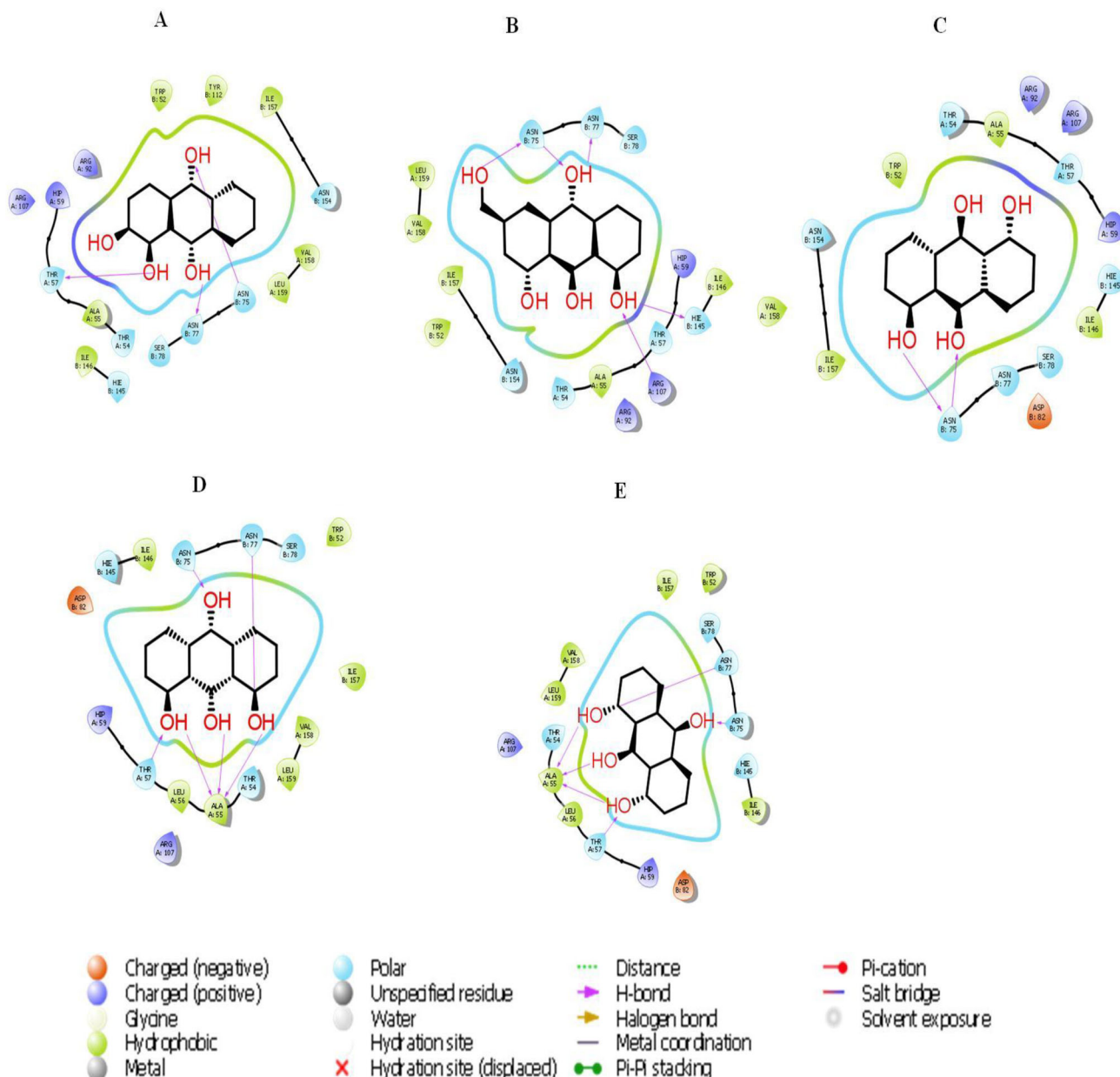


Figure 7. The 2D molecular interactions of best 5 phytochemicals with active site A of 6VYO: (A) Alizarin, (B) Aloe- emodin, (C) Anthrurufin (D), Dantron, (E) Emodin.

phytochemicals; an orally active drug should not violate the rule. Both ligands showed 0 violations for Lipinski's rule of five.

Toxicity predicted by PROTOX-II and admetSAR is summarized in Table 8. Data in Table shows that all the selected phytochemicals are non-carcinogenic and non-cytotoxic in nature and are safe to administer. However, LD₅₀ value of emodin and artemisinin calculated from Protox II was higher than that of all other phytochemicals and chloroquine, indicating that these natural phytochemicals are safer than that of chemically synthesized chloroquine.

MD Simulations of protein-ligand complexes

Among all the 100 phytochemicals, Alizarine, Aloe- emodin and Anthrurufin showed the good binding affinity with

binding site NTD of nucleocapsid protein RNA binding protein of covid-19 (6VYO) and these phytochemicals follows the all parameters (RMSD, RMSF, Intermolecular hydrogen bonding, RoG and Binding free energy through MDS) for molecular dynamic simulation study.

RMSD analysis:

RMSD analysis showed structural stability of protein-ligand complex with in particular time period. Protein-ligand complex behavior upto 50 ns by MDS. The RMSD values of the 6VYO with Alizarine is gradually stabilized at 3 Å and 30 ns and values are same for 50 ns. Similarly, in case of aloe-emodin RMSD value is stabilized at 4 Å and 35 ns and values are same for 50 ns. In case of Anthrurufin RMSD value is stabilized at 3.5 – 4 Å and 45 ns and values are same for 50 ns (Figure 13A).

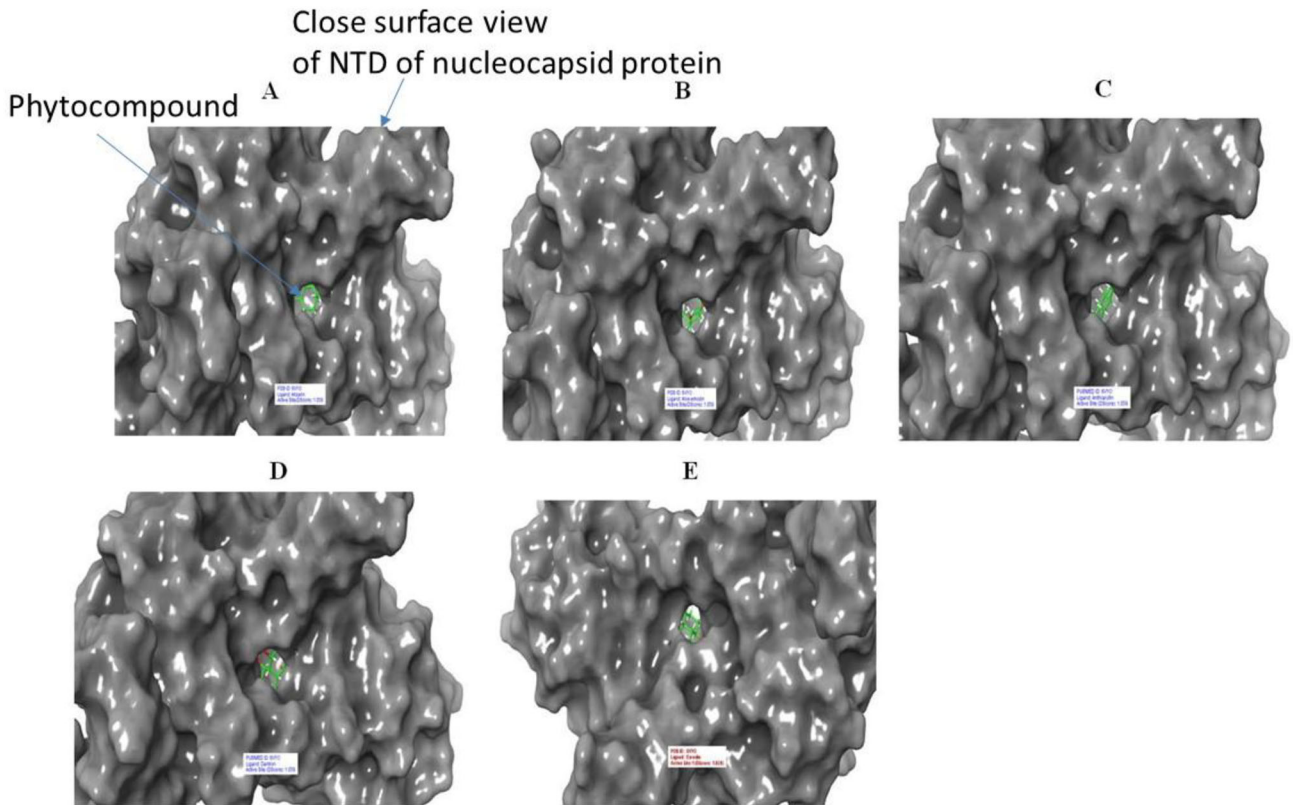


Figure 8. Surface view of 6VYO (active site A) complex with best 5 compounds of selected medicinal plants: (A) Alizarin, (B) Aloe- emodin, (C) Anthrurufin (D), Dantron, (E) Emodin. Phytocompounds are colored in green.

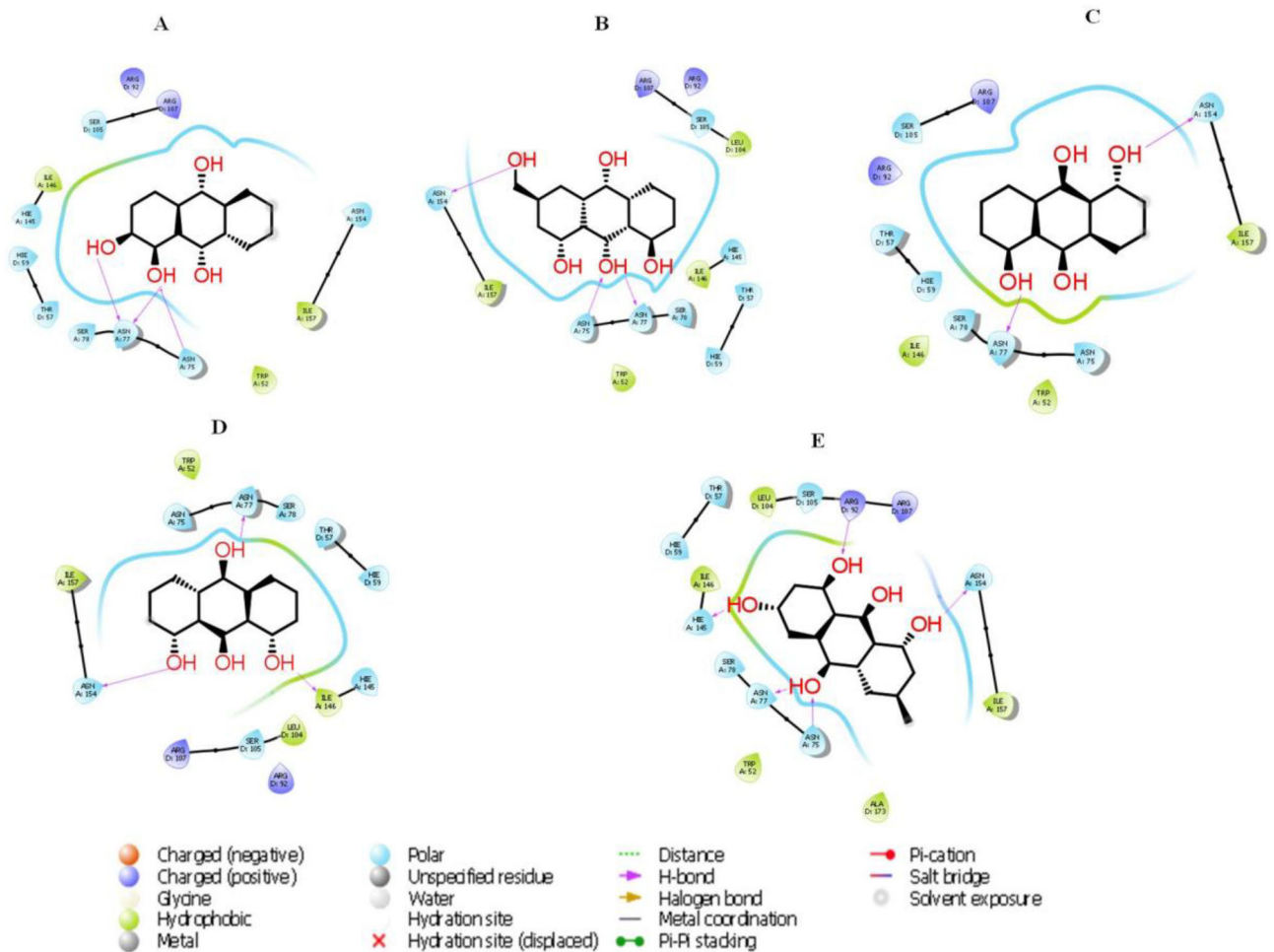


Figure 9. The 2D molecular interactions of best 5 phytocompounds with active site B of 6VYO: (A) Alizarin, (B) Aloe- emodin, (C) Anthrurufin (D) Dantron (E) Emodin.

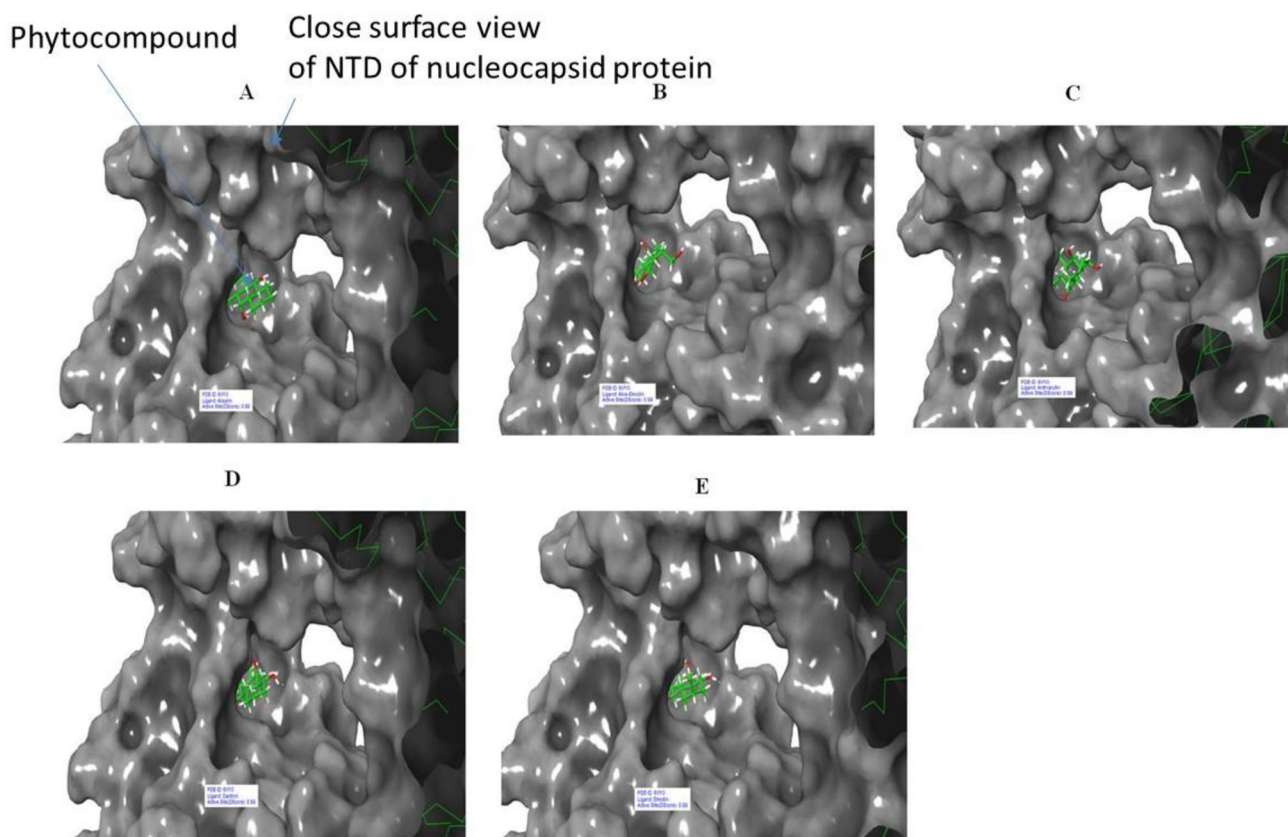


Figure 10. Surface of 6VYO (active site B) with best 5 compounds: (A) Alizarin, (B) Aloe- emodin, (C) Anthrurufin (D) Dantron (E) Emodi. Phytocompounds are colored in green.

RMSF analysis:

The RMSF determines the deviation of the particle from the original position of macromolecules of three dimensional structure of protein. It describes the conformational flexibility of the protein structure. We found the low fluctuation in loop of Alizarine and 6VYO complex; aloe- emodin and 6vyo complex and high fluctuation anthrarufin and 6vyo complex (Figure 13B).

Intermolecular hydrogen bonding analysis

It measures the binding affinity of ligand. Therefore more no. of hydrogen bonds between the protein and Ligands showed strong binding affinity. In this study we found maximum 27 hydrogen bond at the end of 50 ns simulation 23 hydrogen bonds in Alizarine and 22 in aloe- emodin and 24 in Anthrarufin (Figure 14A).

RoG analysis:

It describes the folding competence of the protein- ligand complexes. Through RoG analysis we confirm the conformational changes in the three-dimensional structure of protein after interaction of ligand. The high RoG value showed the loose packing and folding behavior of the protein ligand complex. All the complexes showed the high value at approximately 27.2 Å throughout 50 ns (Figure 14B).

4. Discussion

Molecular docking studies explored the interaction of 100 major phytocompounds of ten selected medicinal plants (*Rheum emodi*, *Thymus serpyllum*, *Cymbopogon citrates*, *Moringa oleifera*, *Thalictrum foliolosum*, *Berberis aristata*, *Piper nigrum*, *Allium sativum*, *Myristica fragrans* and *Zanthoxylum armatum*) for interaction with RNA binding domain (NTD) of nucleocapsid phosphoprotein of SARS coronavirus 2.

The molecular docking study showed that out to 100 different phytocompounds, five phytocompounds such as emodin, anthrarufin, alizarine, aloe- emodin and dantron of *Rheum emodishowed* efficient binding affinity and pharmacokinetic properties with NTD of RNA binding domain of nucleocapsid phosphoprotein of SARS coronavirus 2. It is very interesting to note that all the all the five phytocompounds (emodin, aloe-emodin, anthrarufin, alizarine, and dantron) of *R. emodi* bind at three different active sites. The binding energies of emodin, aloe-emodin, anthrarufin, alizarine, and dantron was -8.299 , -8.508 , -8.456 , -8.441 , and -8.322 Kcal mol $^{-1}$ respectively (site A), -7.714 , -6.433 , -6.354 , -6.598 , and -6.99 Kcal mol $^{-1}$ respectively (site B), and -8.299 , 8.508 , 8.538 , 8.841 , and 8.322 Kcal mol $^{-1}$ respectively (site C). Similar to our study, Kumar et al (Kumar et al., 2020) reported the binding affinities of Nelfinavir, Rhein, Withanolide D, Withaferin A, Enoxacin, and Aloe-emodin as -8.4 , -8.1 , -7.8 , -7.7 , -7.4 , and -7.4 Kcal mol $^{-1}$ respectively against main protease (6LU7) of COVID 19. Latha

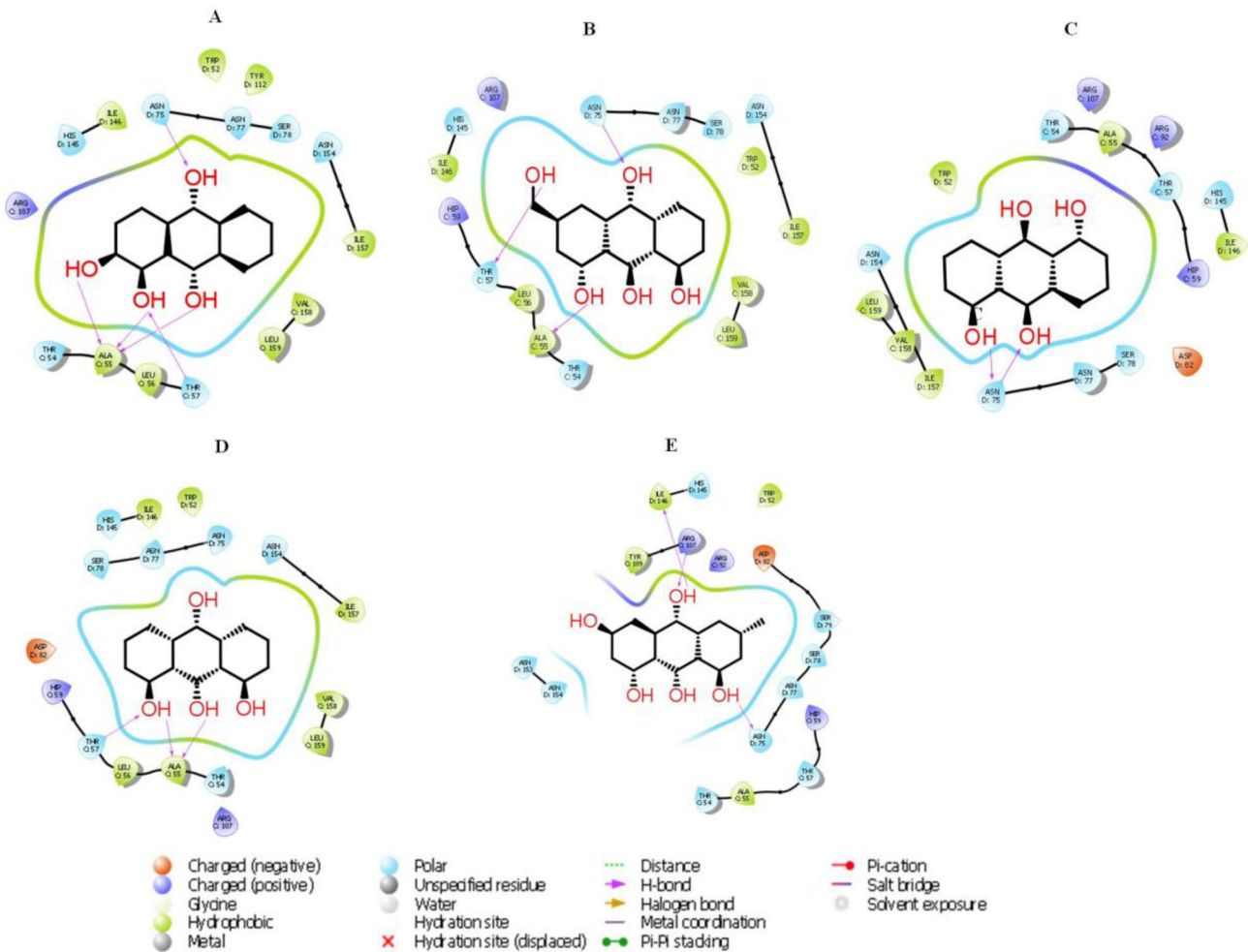


Figure 11. The 2D molecular interactions of best 5 phytochemicals with active site C of 6VYO: (A) Alizarin, (B) Aloe-emodin, (C) Anthrarufin (D) Dantron (E) Emodin. Phytochemicals are colored in green.

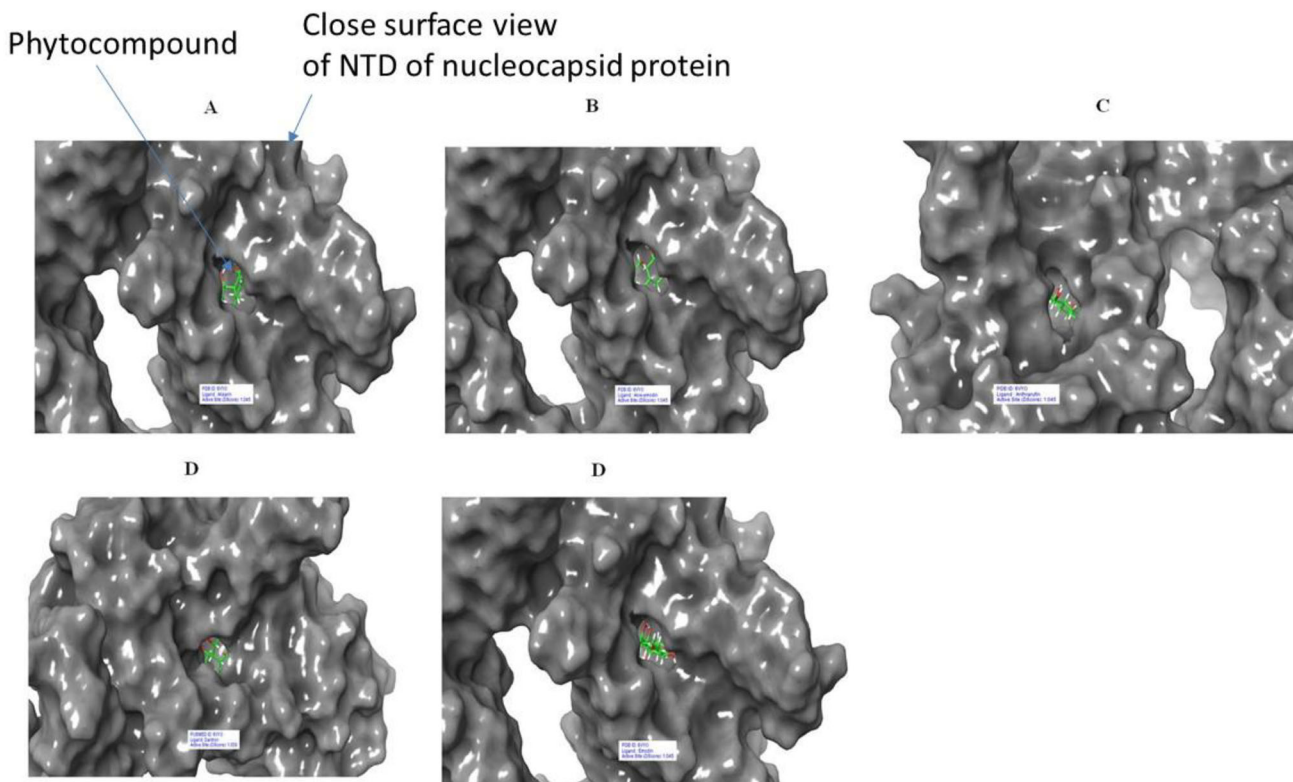


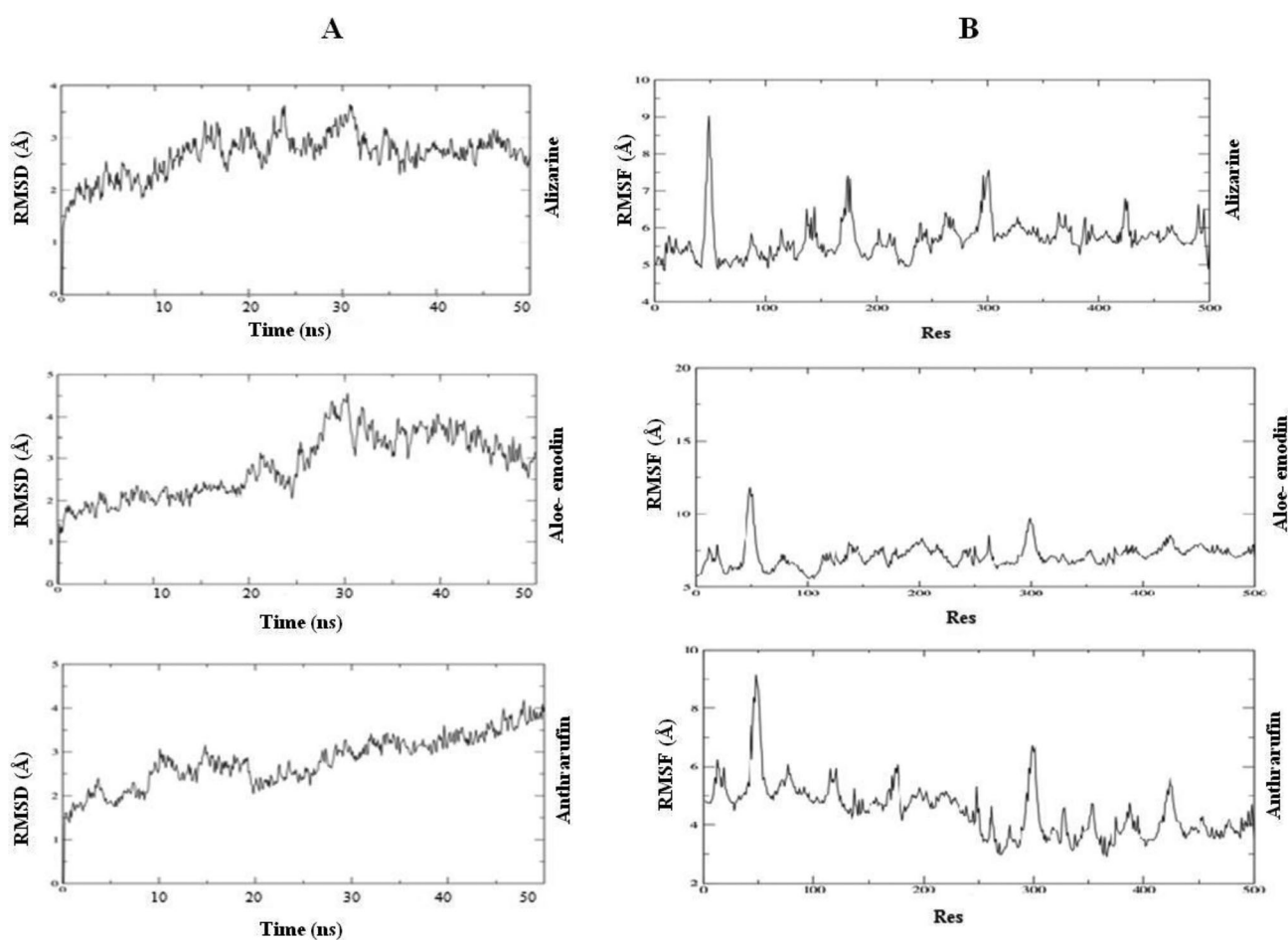
Figure 12. Surface of 6VYO (active site C) and 5 best compounds complex: (A) Alizarin, (B) Aloe-emodin, (C) Anthrarufin (D) Dantron (E) Emodin. Phytochemicals are colored in green.

Table 7. ADME properties of selected phytochemicals predicted by SwissADME.

Compounds	SwissADME											
	Water Solubility	GI Absorption	Drug likeness Rules									
			Lipinski's rule of 5						Ghose	Veber	Egan	Muegge
			Logp	nON	nOHNH	TPSA (Å ²)	MW					
Emodin	Soluble	High	3.01	5	3	94.83	270.24	Yes	Yes	Yes	Yes	
Anthrarufin	Moderately soluble	High	3.13	4	2	74.60	240.21	Yes	Yes	Yes	Yes	
Alizarine	Soluble	High	2.90	4	2	74.60	240.21	Yes	Yes	Yes	Yes	
Aloe- emodin	Soluble	High	2.42	5	3	94.83	270.24	Yes	Yes	Yes	Yes	
Dantron	Soluble	High	3.13	4	2	74.60	240.21	Yes	Yes	Yes	Yes	

Table 8. Toxicity prediction of active phytochemicals predicted by admetSAR and PROTOX-II software.

Phytochemicals	admet SAR		Protox II	
	Carcinogens	Rate Acute toxicity (LD ₅₀) kg mol ⁻¹	LD ₅₀ (mg kg ⁻¹)	Cytotoxicity
Emodin	non-carcinogen	2.5826 (III)	5000 (Class 5)	Inactive
Anthrarufin	Non-carcinogen	2.8601 (III)	5000 (class 5)	Inactive
Alizarine	Non-carcinogen	2.5292 (III)	7000 (class 5)	Inactive
Aloe- emodin	Non-carcinogen	2.9280 (II)	5000 (class 5)	Inactive
Dantron	Non-carcinogen	2.8601 (III)	7000 (class 6)	Inactive

**Figure 13.** A) RMSD graph of three protein-ligand complexes for 50 ns. (B) RMSF graph of three ligand-protein complexes for 50 ns.

and Pandit (Latha & Pandit, 2020) reported the binding affinity of phytochemicals derived from *Silybum marianum* (Silybin), *Withania somnifera* (Withaferin A), *Tinospora cordifolia* (Cordioside) and *Aloe barbadensis* (Catechin and

Quercetin) with SARS-CoV-2 target. The binding energies of phytochemicals was more than the widely used hydroxy-chloroquine and other repurposed drugs used for treatment of COVID-19 infection. Tatar and Turhan (2020) reported the

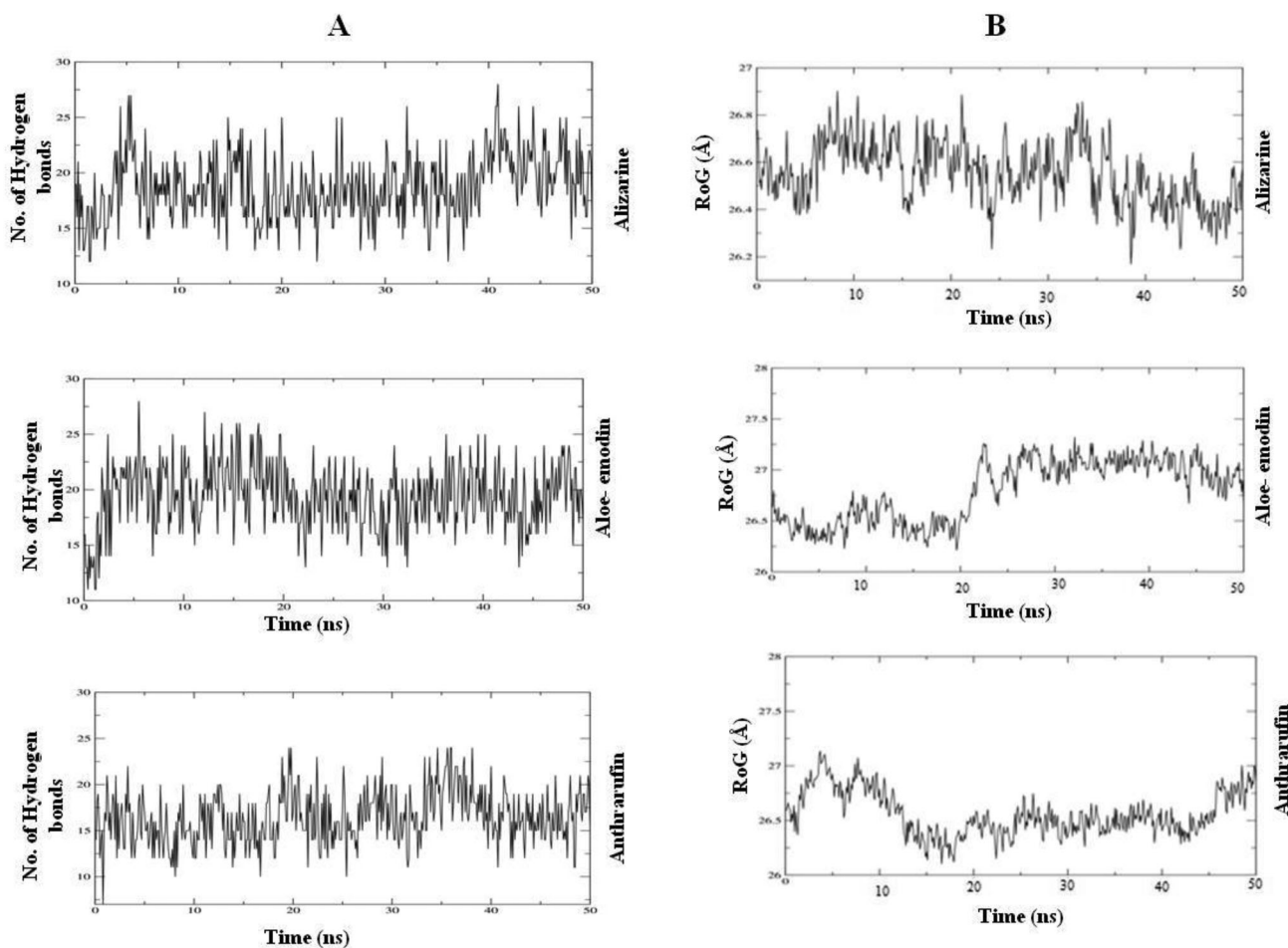


Figure 14. (A) Number of Intermolecular hydrogen bonds between the ligands and amino acid residues of the target protein for 50 ns. (B) Radius of gyration (RoG) results of the ligand-protein complex for 50 ns.

binding affinity of nafamostat, rapamycin, saracatinib, Imatinib and Camostat with binding energy -10.24 , -9.28 , -9.66 , -9.23 and 9.07 respectively with N-Terminal Domain of SARS-CoV-2 Nucleocapsid. Ubani et al. (2020) reported best binding affinity of scopodulcic acid and 249 Dammarenolic acid with the Spike glycoprotein (6VSB) and the Mpro 250 (6FLU7) respectively. The *in-silico* studies were supported by the fact that Schwarz et al. (2011) reported emodin as inhibitor of 3a ion channel of corona virus SARS-CoV and HCoV-OC43 as well as virus release from HCoV-OC43. In another study, Ho et al. (2007) identified emodin as an effective to block the interaction of the SARS-CoV S protein with the ACE2 and the infection by S protein-pseudo-typed retrovirus.

Similar to our study, Ahmed and Shohael (Ahmed & Shohael, 2019), reported that the chrysophanol, aloe-emodin, rhein and emodin fulfill all the criteria of Lipinski's rule of five and ADME/T. Nucleocapsid N protein of SARS coronavirus 2 has been predicted to contain many phosphorylation sites at Serine, Threonine and Tyrosine residues (Davidson et al., 2020). In our study, we found that some of the potential Serine and Threonine residues contribute for the formation of active site A, B and C. Serine at position 78, 79 and 105 also showed interaction with all the five phytocompounds of *R. emodi*. Involvement of potential phosphorylation residues in interaction with phytocompounds could

further ensure that NTD of Nucleocapsid N protein of SARS coronavirus 2 render inactive and prevents the assembly of the virus and hence stop the infection.

5. Conclusion

Hundred phytocompounds of ten medicinal plants were screened on the bases of binding energy against NTD of Nucleocapsid protein of COVID-19 target. Among all the 100 phytocompounds, emodin, Anthrarufin, Alizarine, Aloe-emodin, and Dantron showed the good binding affinity at three different active sites of N-Terminal Domain of SARS-CoV-2 Nucleocapsid Protein and potentially prevent the assembly of virus particles and stop the infection, ADMET prediction revealed that emodin, Anthrarufin, Alizarine, Aloe-emodin, and Dantron are potential drugs for COVID-19 treatment. Molecular dynamic simulation of the three protein-ligand complexes (alizarin, aloe-emodin and anthrarufin) showed stable interaction for 50 ns.

Acknowledgements

The authors acknowledge Shoolini University, Solan (India) for providing infrastructure support to conduct the research work. Authors also acknowledge the support provided by Yeast Biology Laboratory, School

of Biotechnology, Shoolini University, Solan, India. Authors are thankful to the Department of Pharmacology, AIIMS, Rishikesh, Dr. Prajwal Nandekar, Dr. Vinod and Schrodinger team; Dheeraj Kumar Chaurasia from Supercomputing facility for Bioinformatics and Computational Biology, IIT Delhi for their help.

Disclosure statement

The authors declare that they have no conflicts of interest.

References

- Ahmed, S., & Shohael, A. M. (2019). *In silico* studies of four anthraquinones of *Senna alata* L. as potential antifungal compounds. *Pharmacologyonline*, 2, 259–268.
- Aja, P. M., Nwachukwu, N., Ibiham, U. A., Igwenyi, I. O., Offor, C. E., & Orji, U. O. (2014). Chemical constituents of *Moringa oleifera* leaves and seeds from Abakaliki, Nigeria. *Am. J. Phytomed. Clin. Ther*, 2, 310–321.
- Baloch, I. I., Watts, A., Thomas-Bachli, A., Huber, C., Kraemer, M. U., & Khan, K. (2020). Potential for global spread of a novel coronavirus from China. *Travel Med*, 27, e011.
- Banerjee, P., Eckert, A. O., Schrey, A. K., & Preissner, R. (2018). ProTox-II: a webserver for the prediction of toxicity of chemicals. *Nucleic Acids Research*, 46(W1), W257–W263. <https://doi.org/10.1093/nar/gky318>
- Baric, R. S., Nelson, G. W., Fleming, J. O., Deans, R. J., Keck, J. G., Casteel, N., & Stohlman, S. A. (1988). Interactions between coronavirus nucleocapsid protein and viral RNAs: implications for viral transcription. *Journal of Virology*, 62(11), 4280–4287. <https://doi.org/10.1128/JVI.62.11.4280-4287.1988>
- Ben-Shabat, S., Yarmolinsky, L., Porat, D., & Dahan, A. (2020). Antiviral effect of phytochemicals from medicinal plants: Applications and drug delivery strategies. *Drug Deliv Transl Res*, 10(2), 354–367. <https://doi.org/10.1007/s13346-019-00691-6>
- Chen, I. J., Yuann, J. M. P., Chang, Y. M., Lin, S. Y., Zhao, J., Perlman, S., Shen, Y. Y., Huang, T. H., & Hou, M. H. (2013). Crystal structure-based exploration of the important role of Arg106 in the RNA-binding domain of human coronavirus OC43 nucleocapsid protein. *Biochimica et biophysica Acta*, 1834(6), 1054–1062. <https://doi.org/10.1016/j.bbapap.2013.03.003>
- Cong, Y., Ulasli, M., Schepers, H., Mauthe, M., V'kovski, P., Kriegenburg, F., Thiel, V., de Haan, C. A., & Reggiori, F. (2020). Nucleocapsid protein recruitment to replication-transcription complexes plays a crucial role in coronaviral life cycle. *Journal of Virology*, 94, e-01919.
- D., Kumar, V., S., Raj, B. & Rathi, (2020). *In silico* identification of potent FDA approved drugs against Coronavirus COVID-19 main protease: A drug repurposing approach. *Chemical Biology Letters*, 7, 166–175.
- Davidson, A. D., Williamson, M. K., Lewis, S., Shoemark, D., Carroll, M. W., Heesom, K., Zambon, M., Ellis, J., Lewis, P. A., Hiscox, J. A., & Matthews, D. A. (2020). Characterisation of the transcriptome and proteome of SARS-CoV-2 using direct RNA sequencing and tandem mass spectrometry reveals evidence for a cell passage induced in-frame deletion in the spike glycoprotein that removes the furin-like cleavage site. *bioRxiv*, 03.22.002204; <https://doi.org/10.1101/2020.03.22.002204>
- Dev, K., Kumar, V., Rolta, R., & Sharma, A. Herbal Pharmaceutical Excipient for Enhancing Antifungal and Antibacterial Properties of Existing Drugs. Indian Patent Filing Number: 201711028454. (2017).
- Fenwick, G. R., & Hanley, A. B. (1985). Allium species poisoning. *The Veterinary Record*, 116(1), 28. <https://doi.org/10.1136/vr.116.1.28>
- Ganjhu, R. K., Mudgal, P. P., Maity, H., Dowarha, D., Devadiga, S., Nag, S., & Arunkumar, G. (2015). Herbal plants and plant preparations as remedial approach for viral diseases. *Virusdisease*, 26(4), 225–236. <https://doi.org/10.1007/s13337-015-0276-6>
- Georgiev, V., Stefanov, A., & Tarulli, M. (2005). Smoothing-Strichartz estimates for the Schrodinger equation with small magnetic potential. *Journées Équations Aux Dérivées Partielles*, e0509416. <https://doi.org/10.5802/jedp.17>
- Gordon, D. E., Jang, G. M., Bouhaddou, M., Xu, J., Obernier, K., O'meara, M. J., Guo, J. Z., Swaney, D. L., Tummino, T. A., Huttenhain, R., & Kaake, R. M. (2020). A SARS-CoV-2-human protein-protein interaction map reveals drug targets and potential drug-repurposing. *BioRxiv*, <https://doi.org/10.1101/2020.03.22.002386>.
- Grossoehme, N. E., Li, L., Keane, S. C., Liu, P., Dann, C. E., Leibowitz, J. L., & Giedroc, D. P. (2009). Coronavirus N protein N-terminal domain (NTD) specifically binds the transcriptional regulatory sequence (TRS) and melts TRS-cTRS RNA duplexes. *J. Mol. Biol*, 394(3), 544–557. <https://doi.org/10.1016/j.jmb.2009.09.040>
- Gupta, E. (2020). Elucidating the Phytochemical and Pharmacological Potential of *Myristicafragrans* (Nutmeg). In *Ethnopharmacological Investigation of Indian Spices* (pp. 52–61). IGI Global.
- Ho, T. Y., Wu, S. L., Chen, J. C., Li, C. C., & Hsiang, C. Y. (2007). Emodin blocks the SARS coronavirus spike protein and angiotensin-converting enzyme 2 interaction. *Antiviral Research*, 74(2), 92–101. <https://doi.org/10.1016/j.antiviral.2006.04.014>
- Jaric, S., Mitrovic, M., & Pavlović, P. (2015). Review of ethnobotanical, phytochemical, and pharmacological study of *Thymus serpyllum* L. Evid. Based Complement. *Evidence-Based Complementary and Alternative Medicine : Ecamp*, 2015, 101978 <https://doi.org/10.1155/2015/101978>
- Kalyaanamoorthy, S., & Chen, Y. P. (2011). Structure-based drug design to augment hit discovery. *Drug Discov. Today*, 16(17-18), 831–839. <https://doi.org/10.1016/j.drudis.2011.07.006>
- Kang, Y. L., Chou, Y. Y., Rothlauf, P. W., Liu, Z., Piccinotti, S., Soh, T. K., Cureton, D., Case, J. B., Chen, R. E., Diamond, M. S., & Whelan, S. P. (2020). Inhibition of PI3Kγ kinase prevents infection by EBOV and SARS-CoV-2. *bioRxiv*, <https://doi.org/10.1101/2020.04.21.053058>.
- Lanka, G., Bathula, R., Dasari, M., Nakkala, S., Bhargavi, M., Somadi, G., & Potlapally, S. R. (2019). Structure-based identification of potential novel inhibitors targeting FAM3B (PANDER) causing type 2 diabetes mellitus through virtual screening. *Journal of Receptor and Signal Transduction Research*, 39(3), 253–263. <https://doi.org/10.1080/10799893.2019.1660897>
- Latha, N., & Pandit, M. (2020). *In silico* studies reveal potential antiviral activity of phytochemicals from medicinal plants for the treatment of COVID-19 infection. <https://doi.org/10.21203/rs.3.rs-22687/v1>
- Lionta, E., Spyrou, G., Vassilatis, D. K., & Cournia, Z. (2014). Structure-based virtual screening for drug discovery: Principles, applications and recent advances. *Current Topics in Medicinal Chemistry*, 14(16), 1923–1938. <https://doi.org/10.2174/1568026614666140929124445>
- Lo, Y. S., Lin, S. Y., Wang, S. M., Wang, C. T., Chiu, Y. L., Huang, T. H., & Hou, M. H. (2013). Oligomerization of the carboxyl terminal domain of the human coronavirus 229E nucleocapsid protein. *FEBS Letters*, 587(2), 120–127. <https://doi.org/10.1016/j.febslet.2012.11.016>
- Masters, P. S., & Sturman, L. S. (1990). Background paper. Functions of the coronavirus nucleocapsid protein. *Advances in Experimental Medicine and Biology*, 276, 235–238. https://doi.org/10.1007/978-1-4684-5823-7_32
- McBride, R., van Zyl, M., & Fielding, B. C. (2014). The coronavirus nucleocapsid is a multifunctional protein. *Viruses*, 6(8), 2991–3018. <https://doi.org/10.3390/v6082991>
- Meng, Y., Lu, D., Guo, N., Zhang, L., & Zhou, G. (1993). Anti-HCMV effect of garlic components. *Virolog Sin*, 8, 147–150.
- Nai-Lan, G., Cao-Pei, L., Woods, G. L., Reed, E., Gui-Zhen, Z., Li-Bi, Z., & Waldman, R. H. (1993). Demonstration of antiviral activity of garlic extract against human cytomegalovirus in vitro. *Chin. Med. J.*, 106, 93–96.
- Nandekar, P. P., Tumbi, K. M., Bansal, N., Rathod, V. P., Labhsetwar, L. B., Soumya, N., Singh, S., & Sangamwar, A. T. (2013). Chem-bioinformatics and in vitro approaches for candidate optimization: A case study of NSC745689 as a promising antitumor agent. *Medicinal Chemistry Research*, 22(8), 3728–3742. <https://doi.org/10.1007/s00044-012-0364-8>
- Nelson, G. W., Stohlman, S. A., & Tahara, S. M. (2000). High affinity interaction between nucleocapsid protein and leader/intergenic sequence of mouse hepatitis virus RNA. *J. Gen. Virol*, 81(Pt 1), 181–188. <https://doi.org/10.1099/0022-1317-81-1-181>
- Oladeji, O. S., Adelowo, F. E., Ayodele, D. T., & Odelade, K. A. (2019). Phytochemistry and pharmacological activities of *Cymbopogon*

- citratu*: A review. *Scientific African*, 6, e00137. <https://doi.org/10.1016/j.sciaf.2019.e00137>
- Pal, S. K., Mukherjee, P. K., Saha, K., Pal, M., & Saha, B. P. (1995). Antimicrobial action of the leaf extract of *Moringa oleifera* Lam. *Ancient Science of Life*, 14(3), 197–199.
- Potdar, D., Hirwani, R. R., & Dhulap, S. (2012). Phyto-chemical and pharmacological applications of *Berberis aristata*. *Fitoterapia*, 83(5), 817–830. <https://doi.org/10.1016/j.fitote.2012.04.012>
- Ramajayam, R., Tan, K. P., & Liang, P. H. (2011). Recent development of 3C and 3CL protease inhibitors for anti-coronavirus and anti-picornavirus drug discovery. *Biochemical Society Transactions*, 39(5), 1371–1375. <https://doi.org/10.1042/BST0391371>
- Ramatenki, V., Potlapally, S. R., Dumpati, R. K., Vadija, R., & Vuruputuri, U. (2015). Homology modeling and virtual screening of ubiquitin conjugation enzyme E2A for designing a novel selective antagonist against cancer. *Journal of Receptor and Signal Transduction Research*, 35(6), 536–549. <https://doi.org/10.3109/10799893.2014.969375>
- Rolta, R., Kumar, V., Sourirajan, A., Upadhyay, N. K., & Dev, K. (2020). Bioassay guided fractionation of rhizome extract of *Rheum emodi* wall as bio-availability enhancer of antibiotics against bacterial and fungal pathogens. *Journal of Ethnopharmacology*, 257, 112867. <https://doi.org/10.1016/j.jep.2020.112867>
- Rolta, R., Sharma, A., Kumar, V., Sourirajan, A., Baumler, D. J., & Dev, K. (2018). Methanolic Extracts of the Rhizome of *R. emodi* Act as Bioenhancer of Antibiotics against Bacteria and Fungi and Antioxidant Potential. *Med. Plant*, 8, 74–85.
- Saikatendu, K. S., Joseph, J. S., Subramanian, V., Neuman, B. W., Buchmeier, M. J., Stevens, R. C., & Kuhn, P. (2007). Ribonucleocapsid formation of severe acute respiratory syndrome coronavirus through molecular action of the N-terminal domain of N protein. *Journal of Virology*, 81(8), 3913–3921. <https://doi.org/10.1128/JVI.02236-06>
- Sanders, J. M., Monogue, M. L., Jodlowski, T. Z., & Cutrell, J. B. (2020). Pharmacologic treatments for coronavirus disease 2019 (COVID-19): A review. *JAMA*, 323, 1824–1836. <https://doi.org/10.1001/jama.2020.6019>
- Schwarz, S., Wang, K., Yu, W., Sun, B., & Schwarz, W. (2011). Emodin inhibits current through SARS-associated coronavirus 3a protein. *Antiviral Research*, 90(1), 64–69. <https://doi.org/10.1016/j.antiviral.2011.02.008>
- Sharma, N., Kumar, V., Chopra, M. P., Sourirajan, A., Dev, K., & El-Shazly, M. (2020). *Thalictrum foliolosum*: A lesser unexplored medicinal herb from the Himalayan region as a source of valuable benzyl isoquinoline alkaloids. *Journal of Ethnopharmacology*, 255, 112736. <https://doi.org/10.1016/j.jep.2020.112736>
- Singh, M., & Shikha, D. (2017). *Zanthoxylumarmatum* DC: Past, present and future prospective. *Biotech Today : An International Journal of Biological Sciences*, 7(1), 21–24. <https://doi.org/10.5958/2322-0996.2017.00012.6>
- Takooree, H., Aumeeruddy, M. Z., Rengasamy, K. R., Venugopala, K. N., Jeewon, R., Zengin, G., & Mahomoodally, M. F. (2019). A systematic review on black pepper (*Piper nigrum* L.): From folk uses to pharmacological applications. *Critical Reviews in Food Science and Nutrition*, 59(sup1), S210–S243. <https://doi.org/10.1080/10408398.2019.1565489>
- Tan, Y. W., Fang, S., Fan, H., Lescar, J., & Liu, D. X. (2006). Amino acid residues critical for RNA-binding in the N-terminal domain of the nucleocapsid protein are essential determinants for the infectivity of coronavirus in cultured cells. *Nucleic Acids Research*, 34(17), 4816–4825. <https://doi.org/10.1093/nar/gkl650>
- Tatar, G., & Turhan, K. (2020). Investigation of the N-Terminal Domain of SARS-CoV-2 Nucleocapsid Protein with Antiviral Compounds Based on Molecular Modeling Approach. *Science Open Preprints*. <https://doi.org/10.14293/S2199-1006.1.SOR-PPPT991.v1>
- Tripathi, S. K., Muttineni, R., & Singh, S. K. (2013). Extra precision docking, free energy calculation and molecular dynamics simulation studies of CDK2 inhibitors. *Journal of Theoretical Biology*, 334, 87–100. <https://doi.org/10.1016/j.jtbi.2013.05.014>
- Tsai, Y., Cole, L. L., Davis, L. E., Lockwood, S. J., Simmons, V., & Wild, G. C. (1985). Antiviral properties of garlic: In vitro effects on influenza B, herpes simplex and coxsackie viruses. *Planta Medica*, 51(05), 460–461. <https://doi.org/10.1055/s-2007-969553>
- Ubani, A., Agwom, F., Shehu, N. Y., Luka, P., Umera, E. A., Umar, U., Omale, S. E., Nnadi, N. E. & Aguiyi, J. C. (2020). Molecular Docking Analysis of Some Phytochemicals on Two SARS-CoV-2 Targets. *bioRxiv*, <https://doi.org/10.1101/2020.03.31.017657>.
- Weber, N. D., Andersen, D. O., North, J. A., Murray, B. K., Lawson, L. D., & Hughes, B. G. (1992). In vitro virucidal effects of *Allium sativum* (garlic) extract and compounds. *Planta Medica*, 58(5), 417–423. <https://doi.org/10.1055/s-2006-961504>
- Wrapp, D., Wang, N., Corbett, K. S., Goldsmith, J. A., Hsieh, C. L., Abiona, O., Graham, B. S., & McLellan, J. S. (2020). Cryo-EM structure of the 2019-nCoV spike in the prefusion conformation. *Science (New York, N.Y.)*, 367(6483), 1260–1263. <https://doi.org/10.1126/science.abb2507>
- Yadav, R., Imran, M., Dhamija, P., Suchal, K., & Handu, S. (2020). Virtual screening and dynamics of potential inhibitors targeting RNA binding domain of nucleocapsid phosphoprotein from SARS-CoV-2. *Journal of Biomolecular Structure and Dynamics*, 20, 1–6.